BREEDIT: A novel multiplex genome editing strategy to improve complex quantitative traits in maize (*Zea mays* L.)

Christian Damian Lorenzo,[1,2] Kevin Debray,[1,2] Denia Herwegh,[1,2] Ward Develtere,[1,2] Lennert Impens,[1,2] Dries Schaumont,[3] Wout Vandeputte,[1,2] Stijn Aesaert,[1,2] Griet Coussens,[1,2] Yara de Boe,[1,2] Kirin Demuynck,[1,2] Tom Van Hautegem,[1,2] Laurens Pauwels,[1,2] Thomas B. Jacobs,[1,2] Tom Ruttink,[3] Hilde Nelissen,[1,2] and Dirk Inzé[1,2,*,†]

[1] Center for Plant Systems Biology, VIB, B-9052 Gent, Belgium

[2] Department of Plant Biotechnology and Bioinformatics, Ghent University, B-9052 Gent, Belgium

[3] Flanders Research Institute for Agriculture, Fisheries and food (ILVO), B-9820 Merelbeke, Belgium

[*] Author for correspondence: dirk.inze@psb.ugent.be

[†] Senior author

These authors contributed equally (C.D.L., K.D.).

C.D.L. extracted DNA samples, designed and performed the phenotypical experiments, performed crosses and generated the plant material after T1 generation. K.D. analyzed the data and created the visualizations. C.D.L., K.D. and D.I. drafted the manuscript. T.V.H., H.N., D.H. and D.I. selected the candidate genes. W.D., D.H. and T.B.J. designed gRNAs and primers. T.R. curated gene models and initiated the HiPlex sequencing. W.D. and T.B.J. designed, constructed and cloned the SCRIPTs. L.I. and L.P. transformed B104 inbred line to create the EDITOR and SCRIPT lines.

D.S., K.D., and T.R. created bioinformatics pipelines to process and analyze HiPlex sequencing reads. S.A. and G.C. performed the plant transformations, performed initial plant crosses and generated plant material for T0-T1 generation. W.V., Y.B., K.D. assisted with phenotyping, DNA extractions and greenhouse organization. H.N., T.B.J., T.R., L.P. and D.I. initiated and supervised the project.

The author responsible for distribution of materials integral to the findings presented in this article in accordance with the policy described in the Instructions for Author (https://academic.oup.com/plcell) is: Dirk Inzé (dirk.inze@psb.vib-ugent.be).

ORCID IDs: 0000-0003-3954-0234 (C.D.L.); 0000-0003-2898-9415 (K.D.); 0000-0001-7744-6375 (D.H.); 0000-0002-7171-8031 (W.D.); 0000-0002-6330-4744 (L.I.); 0000-0002-4389-0440 (D.S.); 0000-0001-7813-3645 (W.V.); 0000-0001-8787-7347 (S.A); 0000-0003-2285-5782 (G.C.); 0000-0003-3079-2865 (Y.D.B); 0000-0002-8772-3505 (K.D.); 0000-0003-3173-2477 (T.V.H.); 0000-0002-0221-9052 (L.P.); 0000-0002-5408-492X (T.B.J.); 0000-0002-1012-9399 (T.R.); 0000-0001-7494-1290 (H.N.); 0000-0002-3217-8407 (D.I.)

SHORT TITLE: BREEDIT: A novel multiplex genome editing strategy

CORRESPONDING AUTHOR:

Dirk Inzé

Center for Plant Systems Biology

VIB-Ghent University

Technologiepark 71, B-9052 Gent (Belgium).

Tel.: +32 9 3313800; Fax: +32 9 3313809; E-mail: dirk.inze@psb.vib-ugent.be

Abstract

Ensuring food security for an ever-growing global population while adapting to climate change is the main challenge for agriculture in the 21st century. Though new technologies are being applied to tackle the problem, we are approaching a plateau in crop improvement using conventional breeding. Recent advances in gene engineering via the CRISPR/Cas technology pave the way to accelerate plant breeding and meet this increasing demand. Here, we present a gene discovery pipeline named 'BREEDIT' that combines multiplex genome editing of whole gene families with crossing schemes to improve complex traits such as yield and drought resistance. We induced gene knockouts in 48 growth-related genes using CRISPR/Cas9 and generated a collection of over 1000 gene-edited maize plants. Edited populations displayed, on average, significant increases of 5 to 10% for leaf length and up to 20% for leaf width compared with controls. For each gene family, edits in subsets of genes could be associated with increased traits, allowing us to reduce the gene space needed to focus on for trait improvement. We propose BREEDIT as a gene discovery pipeline which can be rapidly applied to generate a diverse collection of mutants to identify subsets of promising candidates that could be later incorporated in breeding programs.

Keywords

Multiplex gene editing; CRISPR/Cas9; multiplex amplicon sequencing; maize; gene family; network engineering; reverse genetics

Introduction

The production of enough food to feed the increasing global population is facing many challenges due to climate change. Extreme temperature ranges, reduction of water availability and limited use of arable land are all expected to converge on a significant drop in crop yields (Zhang and Cai, 2011; Long et al., 2015; Brás et al., 2021). During the past century, conventional breeding has been decisive to adapt crops to local environments and to increase yield under stress conditions (Nuccio et al., 2018; Snowdon et al., 2021). Genomics-assisted breeding has greatly contributed to generate new varieties by incorporating haplotype information in breeding programs (Bhat et al., 2021). Nonetheless, we are slowly approaching a plateau in crop

improvement using conventional breeding, since gene discovery and introgression of favorable alleles cannot be implemented fast enough to cope with the losses caused by environmental stresses.

In that perspective, innovative strategies need to be implemented to bridge the gap between conventional breeding and the knowledge acquired through plant molecular biology to further improve complex traits such as yield. Crop yield is determined by the complex interaction of the (a)biotic environment with the genetically determined growth and developmental processes that drive the plant's life cycle (Elias et al., 2016). There are numerous yield-related traits such as early seedling vigor, root and shoot architecture, biomass allocation, resource use efficiency, senescence, seed filling, etc. In some cases, such as disease resistance, few causative genes control the expression of the trait. However, for many yield- and growth-related quantitative traits (e.g. organ growth, tolerance to abiotic stress such as drought), numerous, small-effect genes contribute (Mickelbart et al., 2015; Poland and Rutkoski, 2016). Traditionally, yield improvement has been tackled from two distinct angles. Breeding aims at producing genetic combinations with better performance, whereas molecular biology works to understand the mode of action of yield-related genes. These two fields operate at very different scales; breeding recombines chromosomal segments towards a favorable genome constitution, whereas molecular biology only deals with a limited number of genes. In crop breeding programs, phenotypes (e.g. seed yield) are collected from many individuals and multi-year/multi-location field trials. By correlating the phenotypes with the genotypic diversity of individuals, genetic variants associated with the improved trait values can be identified (Rasheed et al., 2017). Using this approach, many quantitative agronomic traits have been found to be determined by numerous small-effect loci, with the underlying genomic regions known as 'quantitative trait loci' or QTLs. Such QTLs are generally searched for in segregating mapping populations of recombinant inbred lines (RILs) obtained from two or more parents. A more recent variant of this approach is the genome-wide association study (GWAS), in which numerous genome-wide markers are assayed in many diverse genotypes to associate loci with the phenotypic trait (Wang and Qin, 2017). Furthermore, the combination of phenotypic trait data with the availability of a high number of genomic markers, or even the entire genome sequence, can be used for genomic prediction to increase the predictability of the breeding value of new material (Voss-Fels and Snowdon, 2016). Although these marker-assisted breeding technologies have a major impact on the accuracy and speed of

crop breeding, the genes underlying the QTLs are in many cases unknown. In recent years, technological advances have combined GWAS with molecular -omics phenotypes that go beyond the genomic information, so that molecular networks start to emerge in molecular breeding (Baute et al., 2015; Baute et al., 2016; Xiao et al., 2016; Miculan et al., 2021).

Over the past four decades, there has been tremendous progress in the understanding of the molecular basis of many different plant processes. The use of model organisms such as *Arabidopsis* and rice has been a driving force. A vast amount of research delivered insights into the molecular pathways steering seed development, root growth, leaf development, plant architecture, tolerance to severe drought stress, cold tolerance, flooding and many more agronomic traits. Combined, this information reinforced the idea that plant growth and possibly crop yield may be improved by altering the expression of specific (regulatory) genes. Indeed, many reports have shown that positive effects of yield-related traits could be obtained by modifying the expression of individual genes. In *Arabidopsis*, more than 60 genes were identified that, when ectopically expressed or down-regulated, increase leaf size and in many cases also the size of other organs, including seeds (for reviews, see Gonzalez et al., 2012; Czesnick and Lenhard, 2015; Vercruysse et al., 2020). Likewise, numerous genes that can be used to improve seed yield and size in rice have been identified (Li and Li, 2016). Based on these observations, agro-biotech companies have initiated large-scale programs in the beginning of the 21st century to investigate the effect of numerous selected genes on agronomic traits in crops of interest, mainly maize and rice. The conclusion of these studies was that although positive effects were often noticed in the greenhouse and even in field trials, the observed changes were often too small and too much dependent on the genotype and the environment to justify further investments in pursuing this high-throughput screening approach (Paul et al., 2018; Simmons et al., 2021). Why is it so challenging to translate basic insights in molecular networks and genes into improved crops? In breeding, the phenomenon of expressivity is well-known. Expressivity measures the extent to which a given genotype is expressed at the phenotypic level. The concept of expressivity is best explained by the notion that genes often work in complex networks with many different levels of regulation. Such higher-order regulation is typically exerted on complex and essential processes, such as growth, that need to integrate a panoply of endogenous, genetically determined signals as well as environmental cues. Single-point perturbations of networks often have a limited effect because other components of the network take over to buffer

the system. However, in many cases, the combination of perturbations of a network makes phenotypes much more visible. For example, the pairwise combinations of 13 *Arabidopsis* growth-related genes (GRGs), each enhancing leaf size on their own when ectopically expressed or mutated, lead in more than 80% of the combinations to additive or synergistic effects on leaf size (Vanhaeren et al., 2014; Vanhaeren et al., 2017). Moreover, a triple combination of three different mutants of GRGs increased the size of leaves, flowers, seeds and even roots of Arabidopsis in a spectacular manner (Vanhaeren et al., 2017). Also in maize, albeit with fewer genes, pairwise combinations of specific alleles of growth-enhancing genes result in additive effects (Sun et al., 2017; Liu et al., 2021). This concept is also clearly observed during breeding, when yield traits most often are determined by many small-effect loci that need to work in concert to obtain a maximal output.

Despite the spectacular advances made by systems biology in integrating large data sets, the mechanisms behind the control of plant developmental processes are so complex that predicting which combination of genes would provide the optimal effect on yield remains virtually impossible. Understanding the mode of action might be the best way forward to estimate the combinability of genes (Vanhaeren et al., 2014; Sun et al., 2017). However, even when dealing with a relatively small number of genes, testing all possible pairwise gene combinations remains cumbersome and resource intensive. The investments become even more important when triple or higher-order gene combinations have to be tested, which is necessary to achieve stable yield increases of 10% or higher.

The clustered regularly interspaced short palindromic repeat (CRISPR) technology emerged as a powerful tool for simultaneously multiplex-targeting several GRGs, easily generating genetic variability in a broad set of targets and thus enabling a plethora of combinatorial mutations to be analyzed (Knott and Doudna, 2018; Zhang et al., 2019). Several studies showed how CRISPR could be used to reshape plant architecture and target complex traits in multiple species like tomato (Rodríguez-Leal et al., 2017; Wang et al., 2021), wheat (Li et al., 2020), rice (Meng et al., 2017) and in maize (Doll et al., 2019). As a broader application, large-scale CRISPR screens have been carried out in rice (Lu et al., 2017), cotton (Ramadan et al., 2021), maize (Liu et al., 2020; Gong et al., 2022), tomato (Jacobs et al., 2017), oilseed rape (Li et al., 2018) and soybean (Bai et al., 2020).

Here, we explored an experimental approach to bridge the gap between conventional breeding and genetic engineering of multiple genes by combining multiplex CRISPR-mediated genome editing with crossing schemes to observe favorable phenotypes. We denominated this approach BREEDIT, a contraction of breeding and gene editing, and propose this strategy as a powerful technique to engineer complex traits by knocking out a large number of key players in gene families and pathways. In just two generations, we generated a list of putative gene knockouts (KOs) required to evoke clear yield-related phenotypes in maize. BREEDIT could therefore be used to rapidly identify a subset of genes involved in the expression of a complex trait and identify targets for plant breeding programs.

Results

Development of a CRISPR/Cas9 multiplex genome editing pipeline in maize: general outline

The aim of this study was to develop a flexible pipeline that combines multiplex gene editing and different crossing schemes to generate plants with modified traits (Figure 1). First, 48 candidate GRGs (Table 1) were selected based on the literature or in-house knowledge, in the target species maize, complemented with other model organisms, i.e. *Arabidopsis* and rice (Figure 1A). For instance, negative growth regulators whose inactivation is likely to result in positive effects on growth are suitable GRG candidates. Guide RNAs (gRNAs) targeting these GRGs are designed and cloned into multiplex gene editing vectors (referred to as SCRIPTs), which are then used to transform *Cas9*-expressing lines (named EDITOR lines), resulting in super transformed lines that harbor both Cas9 and a SCRIPT containing 12 gRNAs (Figure 1B; Supplemental Figure S1). The BREEDIT pipeline then uses highly multiplex (HiPlex) amplicon sequencing combined with the SMAP haplotype-window bioinformatics workflow to routinely monitor gene edits at gRNA cutting sites. Amplicon sequencing at great depths enables to collect haplotype sequences and their respective frequencies (Figure 1D). Both types of information can be used to assess the effect of mutations on the encoded protein function or activity and assign a genotype to the plant for a specific locus. Per sample and per locus, the length difference between a mutated haplotype and the reference haplotype is used to classify the mutated haplotypes in two categories: haplotype$_{KO}$ corresponds to haplotypes containing out-frame insertions or deletions (indels), leading to a gene KO and an nonfunctional protein; haplotype$_{REF}$ includes haplotypes with only

single-nucleotide polymorphims (SNPs) outside the cutting site or in-frame indels supposed to have less impact on the translated protein that may still behave as the reference protein. In CRISPR/Cas9 experiments, one plant may contain more haplotypes than its ploidy level because of mosaic tissues as a consequence of the initial (T0) or ongoing (T1, T2) Cas9 activity, thus complicating the genotyping. To interpret complex haplotype constitutions, the relative fraction of all $haplotype_{KO}$ is summed per locus per sample. The resulting aggregation is interpreted as a gene loss-of-function (LOF) dosage, further discretized in three categories: $LOF_{0/2}$ (none of the two chromosomes is affected by a set of $haplotype_{KO}$), $LOF_{1/2}$ (one of the two chromosomes is affected by a set of $haplotype_{KO}$), and $LOF_{2/2}$ (both chromosomes are affected by a set of $haplotype_{KO}$). The three dosage categories are used in genotype-to-phenotype associations.

After selecting transgenic lines, T0 lines are genotyped and the T0 plants with the highest numbers of gene KOs (either partial ($LOF_{1/2}$) or complete ($LOF_{2/2}$)) are crossed to obtain material for phenotyping (Figure 1C). Different crosses can be performed to maximize the number of edited genes as well as to fix combinations of gene edits. Self-crosses serve to fix edits in parallel to maximize phenotypic readout, while backcrosses to the original line provide heterozygous lines which can later be self-crossed and phenotyped in T2. Additional specific crosses can be performed to further enrich edit diversity. Plants harboring the same SCRIPT but containing edits at different genes from that SCRIPT can be crossed to increase the number of gene edits (up to 12) in the corresponding gene family or pathway. Such crosses will be further referred to as intra-script crosses. Furthermore, plants transformed with different SCRIPTs can be crossed to maximally combine mutants in genes covered by different families or pathways. These crosses will be further referred to as inter-script crosses. Since Cas9 remains active in all subsequent generations (Impens et al., 2022), new transgenerational edits are expected to accumulate, resulting in a large collection of higher-order mutants (up to 24 gene edits when two SCRIPTs are combined) in different segregating states (i.e. $LOF_{0/2}$, $LOF_{1/2}$ or $LOF_{2/2}$).

Because several plants are generated following the BREEDIT approach, easy-to-measure quantitative traits are used to maximize the throughput of the phenotyping steps. Despite the high number of plants generated, each individual has likely a unique genotypic profile given the many combinations of indels and dosage that can happen in a set of 12 genes or more. Therefore, repetitions of same genotypic combinations cannot be used for statistics in BREEDIT. The effects of combinations of gene edits on traits are better appraised at the population level, though

the specific causative gene combination cannot be deduced. The effect of a single gene on a trait can however still be evaluated considering that multiple observations of a single gene KO would conceal the putative noise brought by mutations in other genes. The framework for phenotyping experiments consists of several (minimum two) independent trials to test the performance of independent mutated populations compared with the EDITOR line. Single-gene associations to a trait are then conducted per experiment per population. The number of times a gene KO is significantly associated with a trait across different independent populations and experiments is a measure for the importance of that gene in the expression of the trait. At the end of the BREEDIT pipeline, genes can be ranked to delineate a minimal set of candidate genes with maximal effect on trait expression, thus reducing the gene space to be considered for further research.

Applying the BREEDIT strategy

To test the BREEDIT strategy, we selected 48 maize GRGs with potential positive effects on growth when mutated, individually or in combination (Table 1). The gRNAs targeting the 48 genes were distributed over SCRIPT 1 to SCRIPT 4 and were, as much as possible, grouped per gene family. This distribution primarily aims to simultaneously knockout multiple members of the same gene family/pathway to overcome potential functional redundancy of paralogs. In addition, grouping by family aims to generate segregating mutants with a range of gene KOs, which may help to untangle complex relationships in gene regulatory networks that might be overlooked when only single or double mutants are considered. Additionally, chromosomal positions of the GRGs were taken into consideration to spread the distribution of genes belonging to a same SCRIPT over chromosomes when possible (Supplemental Figure S2). The 12 genes targeted in SCRIPT 1 are major players in gibberellin catabolism and signaling. The 12 genes targeted in SCRIPT 2 are maize orthologs of genes encoding cytokinin oxidases (*CKXs*), key regulators of cytokinin catabolism. SCRIPT 3 contains gRNAs for eight genes encoding the family of inhibitors of cyclin-dependent kinase/Kip-related proteins (*ICK/KRP*), as well as four genes expected to encode negative regulators of growth under drought conditions: two maize *PP2C* orthologs (*ZmPP2Cs*) and two *HOMEOBOX*-type genes (*HB124B and HB124C*), orthologs of the *Arabidopsis* genes *PHABULOSA* and *PHAVOLUTA* (McConnell et al., 2001). Finally, SCRIPT 4 contains gRNAs for seven orthologs of class II *CINCINNATA-TEOSINTE BRANCHED 1/CYCLOIDEA/PROLIFERATING CELL FACTOR (CIN-TCP)* and three members

of the *GROWTH REGULATING FACTORS* (*GRF)* genes, major regulators of cell division, leaf shape and leaf size determination. Additionally, gRNAs targeting an ortholog of the GAGA-binding protein-encoding *BASIC PENTACYSTEINE 6* (*ZmBPC6*) and a gene encoding a plant homeodomain (PHD)-finger protein (*ZmPHD8*) were included in SCRIPT 4.

Generation of highly edited maize populations for all SCRIPTs

We developed a set of three independent homozygous EDITOR lines that constitutively express the Cas9 protein in the maize inbred line B104 (Supplemental Figure S3) to execute editing at loci targeted by arrays of 12 gRNAs expressed from the SCRIPT vector. EDITOR 1 and EDITOR 3 were supertransformed with SCRIPT 1 for a preliminary evaluation of gene editing. After transformation, the EDITOR 1 and EDITOR 3 supertransformed populations showed similar editing profiles (Supplemental Figure S4). At T0, six out of the 12 targeted genes showed $LOF_{1/2}$ or $LOF_{2/2}$ in both EDITOR lines and the number of mutant alleles at each locus was comparable between both EDITOR backgrounds. The same gRNAs were active in both EDITOR backgrounds but four genes out of the six being commonly edited in both EDITOR backgrounds have $LOF_{2/2}$ in EDITOR 1 whereas two in EDITOR 3 (Supplemental Figure S4). We proceeded with EDITOR 1 as the genetic background for further experiments and supertransformed this line with the remaining three scripts. Like for SCRIPT 1, we monitored gene edits in T0 plants and all subsequent generations using HiPlex amplicon sequencing. Indels in haplotype sequences ranged from -90 bp to +92 bp. Insertions of one nucleotide (+1 bp) were the most represented type of mutation, but overall, deletions were more present than insertions (Figure 2A). The largest insertions showed sequence similarity to genomic fragments located up to 1 kb upstream or downstream of the expected cutting site. At T0, we detected $haplotype_{KO}$ in 11, 12, 8, and 12 out of the 12 target sites for SCRIPT 1, 2, 3, and 4, respectively (Figure 2B). Across all T0 SCRIPT populations, a large diversity of haplotypes (109 haplotypes with in-frame and 407 haplotypes with out-frame indels) could be identified (Supplemental Figure S5). Some $haplotype_{KO}$ were initially not detected at T0, but appeared in T1 populations (Figure 2B) of both intra-script and inter-script crosses, revealing either ongoing gene editing in subsequent generations or overlooked edits due to mosaic tissues in T0. Overall, from T0 to T2, mutations could be found in all the 48 targeted genes, except one (*SPY* in SCRIPT 1). We focused on $haplotype_{KO}$, and observed a diversity of $haplotype_{KO}$ combinations per locus per sample (mono-, bi-, multi-allelic)

in the T0 to T2 samples, all expected to lead to a gene LOF, either partial ($LOF_{1/2}$) or complete ($LOF_{2/2}$) (Figure 2C). We observed a typical tri-modal distribution for the aggregated fraction of $haplotype_{KO}$ that could be roughly divided into three areas with higher counts, each corresponding to a discrete genotypic class ($LOF_{0/2}$, $LOF_{1/2}$, and $LOF_{2/2}$; Supplemental Figure S6).

From haplotype frequencies to genotypic information

The aggregated fraction of $haplotype_{KO}$ in sequencing reads was used as a proxy to characterize partial ($LOF_{1/2}$) and complete ($LOF_{2/2}$) gene KOs (Figure 3). Our approach for the detection of gene edits using HiPlex amplicon sequencing combined with SMAP haplotype-window analyses successfully captured haplotype sequences in 96% of the cases, encouraging us to use this technique to monitor edits in the offspring (Figure 3A). At T0, 73% (35/48) of the target loci showed $LOF_{1/2}$ or $LOF_{2/2}$, with SCRIPT 1 and SCRIPT 3 performing less than SCRIPT 2 and SCRIPT 4 (Figure 3B). At T1, of the 13 remaining genes not edited at T0, 12 (92%) were *de novo* edited. No $haplotype_{KO}$ was observed at the last remaining non-edited locus (*SPY*) at T2. Also, all the transgenerational *de novo* edits were only heterozygous mono-allelic mutations (Figure 3B). Considering both T0 and T1 materials, we observed plants stacking up to nine $LOF_{1/2}$ or $LOF_{2/2}$ in both SCRIPT 1 and SCRIPT 3, and 11 of $LOF_{1/2}$ or $LOF_{2/2}$ gene KOs in SCRIPT 2 and SCRIPT 4 (Figure 3C). Because of sterility issues, progeny of SCRIPT 1 was difficult to generate by crossing, resulting in the low numbers of T2 for that SCRIPT (Figure 3C). Finally, we also studied progeny resulting from inter-script crosses involving two SCRIPTs (2 × 12 target loci) and observed that, on average, 40% of the loci showing edits in the progeny presented transgenerational editing patterns and 25% were completely *de novo* edited, meaning that edits at these loci were not observed in the parental lines (Supplemental Figure S7). Per locus across all populations, on average 7% of the progeny is affected by transgenerational edits inducing $LOF_{1/2}$ at the target sites.

In conclusion, the approach of supertransforming EDITOR lines with SCRIPT constructs generated a high frequency of heritable edits in T0 and additional transgenerational edits in T1 and T2.

T1 single-SCRIPT multiple-edited populations display phenotypic variability in seedling growth-related traits

After we generated the single-SCRIPT populations of edited plants, we studied the effects of multiple gene edits on plant growth by phenotyping T1 maize seedlings derived from T0 selfings of each SCRIPT at the V3 stage. To facilitate high-throughput phenotyping of several populations, we scored easy-to-measure parameters such as the final leaf length and width of leaf 3 (FLL3 and FLW3, respectively) and also integrative parameters such as the fresh weight (FW), dry weight (DW) and moisture content of plants grown under well-watered (WW) and water-deficient (WD) conditions. We scored populations derived from independent transgenic events to analyze the effect of combinations of LOF dosages resulting from different haplotype$_{KO}$ on trait expression (Figure 4, gradient of edits displayed in orange). Detailed information of the different populations that were phenotyped is provided in Supplemental Table S1.

SCRIPT 1 plants were tested in two independent WW experiments (WW001 and WW008) (Figure 4A, B) and displayed conspicuous phenotypes such as a slender shoot architecture (Figure 4C) with longer and narrower leaves (Figure 4A-B, E) compared with EDITOR 1 controls. The most conspicuous phenotypes could be observed in population P013, which includes individuals with partial or complete LOF in a set of 11/12 genes (Figure 4A-E). Additionally, some SCRIPT 1 plants displayed abnormal tassel development with a lack of florets or pollen and the formation of silks in the anthers (Supplemental Figure S8), leading to male sterility.

For SCRIPT 2 and SCRIPT 3, when tested in experiment WW001, significant increases of about 5% relative to controls could be detected only for FLL3 and only in one of the two populations of each group (P108 for SCRIPT 2, and P033 for SCRIPT 3), while FLW3 remained unaffected in SCRIPT 2 populations or decreased for both populations of SCRIPT 3 (Supplemental Figure S9B-C). Because the genes targeted in SCRIPT 2 are involved in cytokinin metabolism, previously implicated in drought tolerance (Rida et al., 2021), and some of the genes targeted in SCRIPT 3 are drought responsive (Li et al., 2016; Hai et al., 2020), these populations were phenotyped under WD conditions (Supplemental Figure S9B-C). Under WD, the SCRIPT 2 populations showed an enhanced growth (Supplemental Figure S10A), which is reflected by a significant increase in FLL3, FLW3, FW and DW compared with control EDITOR 1 (Supplemental Figure S9B, Supplemental Figure S10 A-C). For SCRIPT 3, all tested populations

353 displayed enhanced growth traits (Supplemental Figure S11), but only significant increases in
354 FLL3 compared with EDITOR 1 were observed (Supplemental Figure S9C). Moreover,
355 population P034 presented a significant increase for FW compared with EDITOR 1 controls
356 (Supplemental Figures S9C and S11).

357 Changes in leaf morphology were also observed for SCRIPT 4 plants (TCP, GRF family
358 genes). Individuals that segregate LOF dosages in 12/12 and 9/12 genes were observed in
359 populations P059 and P060, respectively (Figure 4F-G, gradient of edits in orange; Supplemental
360 Table S1). Both populations presented significantly longer FLL3 (Figure 4F) alongside a >15%
361 increase in FLW3 compared with EDITOR 1 (Figure 4G-I). The increase in FLL3 could not be
362 detected in populations P054, P079, and P130 (Figure 4F, Supplemental Table S1) but the rise in
363 FLW3 was significantly detected in all populations (Figure 4G).

364

365 **Crossing plants with different SCRIPTs allows combining phenotypes in T2 plants**

366 After focusing on single-SCRIPT populations, we phenotyped inter-script populations that stack
367 edits in genes from different SCRIPTs after crossings. For this, T0 plants with different scripts
368 were crossed and the resulting T1 plants (inter-script crosses) were self-crossed. Of all the
369 different combinations, we phenotyped two T2 inter-script populations which presented different
370 profiles of edits in crosses between SCRIPT 2 × SCRIPT 4 (P148 and P152) and SCRIPT 3 ×
371 SCRIPT 4 (P157 and P158) under WD conditions. For both populations of SCRIPT 2 ×
372 SCRIPT 4 and SCRIPT 3 × SCRIPT 4, we detected a significant increase in FLW3
373 (Supplemental Figure S12, and Supplemental Table S1), a phenotype observed in single-
374 SCRIPT 4 T1 lines. For the other traits, distinct differences were observed in each population.
375 P148 displayed an increase in FLL3, whereas P152 showed a decrease in FLL3 and significant
376 increases in FW and moisture content compared with the EDITOR 1 control (Supplemental
377 Figure 12A). Both P157 and P158 displayed significant increases in moisture content and P158
378 displayed reduced DW compared with the EDITOR 1 control (Supplemental Figure 12B).

379

380 **Genotype-to-phenotype associations and gene space reduction**

381 After phenotypic evaluation of all SCRIPT populations, we attempted to determine the possible
382 causative genes for the observed phenotypes. Because each individual phenotyping experiment

did not allow for sufficient replication of LOF dosages combinations, we performed genotype-to-phenotype associations at the single-gene level. For each gene and trait, we compared the three classes of LOF dosages ($LOF_{0/2}$, $LOF_{1/2}$, and $LOF_{2/2}$) with the EDITOR 1 control. Such single-gene analyses were carried out separately for all experiments conducted under WW and WD, representing in total a collection of more than 1000 plants that include data on selfed, inter- and intra-script crossed lines. Our goal here was to detect major gene effects.

Following this approach, we could detect a subset of genes for each gene family which could be, at least partially, significantly responsible for the observed phenotypes (Figure 5). In SCRIPT 1, phenotypes regarding increases in FLL3 and decreases in FLW3 were associated with edits on DELLA orthologs *D8* and *ZmSLR2* as well as on *ZmGa2ox5* (Figure 5A). For SCRIPT 2, edits in *ZmCKX4B*, *ZmCKX6* and *ZmCKX8* were related to changes in FW, FLW3 and DW (Figure 5B). In the case of SCRIPT 3, LOFs in *ZmKRP5-2* and *ZmPP2C-A11* were associated with increases in FW and DW, while LOF in Zm*KRP1-1*, *ZmHB124B* and *ZmHB124* correlated with increases in biomass moisture (Figure 5C). Finally, for SCRIPT 4, the main genes involved in the increases observed in FLW3 were *ZmTCP8*, *ZmTCP9*, *ZmTCP10*, *ZmTCP22* and *ZmTCP42* (Figure 5D). Particularly, LOFs in *ZmTCP22*, *ZmTCP42* and *ZmTCP9* were associated with concomitant increases in FW and moisture content, and therefore decreases in DW. *ZmGRF10* and *ZmGRF4* were associated to increases in FLL3.

To further validate the rationale used for the associations, we analyzed in detail population P012 of SCRIPT 1 (Figure 6). In this population, *D8*, one of the selected genes associated to increases in FLL3 (Figure 5A), showed two $haplotype_{KO}$, each with an out-frame indel (-1 bp and +1 bp) and an $haplotype_{REF}$ with an in-frame indel (-3 bp) (Figure 6A). In the progeny, the haplotypes segregated resulting in different LOF dosage combinations. Within that population, plants containing only a $LOF_{1/2}$ in *D8* presented similar phenotypes of FLL3 and FLW3 compared with EDITOR 1, whereas plants with a $LOF_{2/2}$ in *D8* displayed longer and narrower leaves (Figure 6B-C).

Discussion

Complex agronomical traits such as yield or resistance to a particular (a)biotic stress are governed by a large network of genes that together determine a specific phenotype. Understanding the complexity of such networks is the central aspiration of systems biology.

Here, we developed an experimental approach, named BREEDIT, to study gene networks affecting complex quantitative traits by combining multiplex CRISPR-mediated gene editing of whole gene families with specific crossing schemes. In BREEDIT, a Cas9-expressing line (EDITOR) is supertransformed with vectors containing 12 gRNAs (SCRIPTs) targeting a set of GRGs. Gene edits are further stacked in plants using crossing schemes.

We evaluated the BREEDIT strategy by targeting putative players in major plant gene families or pathways involved in growth regulation. The success rate of the multiplex gene editing approach in maize was very high, with more than 97% of the genes showing at least partial or complete LOF at T1. In just two generations, BREEDIT created multiple gene KOs leading to a diverse collection of genetic profiles, from low-order mutants with one, two or three gene KOs to higher-order mutants stacking mutations on up to 11 genes out of the 12 within a single SCRIPT. Additional levers could be used to further increase the number of gene KOs stacked in one plant, namely inter-script crosses and the ongoing Cas9 activity. We indeed showed that higher-order mutants could be obtained by crossing plants already containing high numbers of gene KOs at the single-SCRIPT level. Finally, the combined presence of the Cas9 and the SCRIPT throughout the generations enabled the CRISPR/Cas9 machinery to continuously generate mutations in not yet edited loci. This ongoing Cas9 activity can therefore contribute to reach saturation in gene edits after a couple of generations and increase the number of gene KOs stacked in one plant. Interestingly, we noticed that while in the T0 plants often both copies of the target genes carried the same or a different mutation (bi-allelic), genes newly edited at T1 all showed heterozygous mutations, suggesting that only one chromosome of the two is edited. We hypothesized that chromatin condensation may influence DNA accessibility for the CRISPR/Cas9 machinery, possibly by imprinting (Borg and Berger, 2015). Further research is needed to elaborate on the mechanisms.

We obtained more than 1000 plants with often different unique LOF profiles to score for phenotypes. The high sensivity of HiPlex amplicon sequencing enabled to capture complete sets of haplotypes with CRISPR/Cas9 mutations in large arrays of samples and loci. We used the haplotype sequence to focus on haplotypes supposed to have major effect ($haplotype_{KO}$) on the translated protein function or activity. The experimental set-up based on multiple observations of significant single-gene KO associations with phenotypes across different populations and experiments enabled us to identify significant phenotypic responses in growth traits for all

SCRIPTs. In the case of SCRIPT 1, we observed previously known effects of elevated gibberellic acid (GA) levels, such as plants with long and narrow leaves (Nelissen et al., 2012; Voorend et al., 2016) as well as male sterility, a trait that was previously associated with the effect of GA on tassel development (Colombo and Favret, 1996). SCRIPT 4 plants displayed an increased FLW3 (alongside with milder increases in FLL3), which impacted the FW in some populations. Lastly, for SCRIPT 2 and SCRIPT 3, the most pronounced phenotypes observed were increased FLL3 and FW, particularly under WD conditions.

If we consider these single-SCRIPT lines as building blocks, the possibility to stack several different combinations of SCRIPTs by crossing, opens the way to create higher-order mutant lines that may display even stronger or additive phenotypes. The inter-script lines we generated displayed higher-order mutations more than (12) and inherited traits observed in parental single-SCRIPT lines. Though some of the expressed traits (e.g. increases in FW) were not observed in all different inter-script populations of the same type (probably because different haplotypes are segregating in different populations), some other traits (such as increases of FLW) were consistently observed in all generations of lines containing SCRIPT 4, which further validates the consistency of the results analyzed at single-SCRIPT level.

Another important outcome of the BREEDIT strategy is the possibility to screen large sets of genes that are then ranked and prioritized to delineate a minimal set of LOF required to induce a maximal phenotypic effect. Further inspection of the selected 48 GRGs showed that certain subsets of genes are strongly associated to specific traits (or combination of traits). Using this information, we built a possible regulatory network that integrates all the single-gene effects and their impact over all the different measured traits (Figure 7). In this network, central genes (such as *ZmCKX4B, ZmCKX48 and ZmCKX46* and *ZmTCP9*, *ZmTCP10*, *ZmTCP22* and *ZmTCP42*) act as nodes connected to several traits, inferring a possible broader role in regulation. The genes located at the edge of the network may play a more defined role, connecting to just one or two traits (such as *ZmGRF10*, *ZmGRF4, ZmCKX3* and *ZmTCP8*). Finally, other genes connect to specific patterns, like *D8*, *SLRL2*, and *Ga2ox5*, of which LOF strongly increases the FLL3 while also strongly decreasing the FLW, or *ZmHB124B*, of which LOF influences the FW and moisture positively. Therefore, using single-gene KO associations, we could identify subsets of genes per family, of which LOF, alone or in combination, may be responsible for the observed phenotypes. Furthermore, some of these genes were already shown to play roles in modifying agronomical

traits in other studies. A gain-of-function mutation in *D8* (SCRIPT 1), encoding a DELLA maize protein ortholog, is causative of dwarf phenotypes (Winkler and Freeling, 1994; Lawit et al., 2010). Zm*CKX-4B* (SCRIPT 2) plays a role in both drought (Rida et al., 2021) and heat shock stress (Wang et al., 2020). Downregulation of *ZmHB124B* and *ZmHB124C* induces the formation of additional protoxylem files in the vasculature (Bloch et al., 2019), which could prevent vascular embolism and water retention under water-limiting conditions (Hwang et al., 2016). *ZmGRF10* (SCRIPT 4) overexpression in maize leads to a decrease in leaf length and height (Wu et al., 2014; Nelissen et al., 2015). Although these genes were highlighted in our single-gene KO associations, we cannot exclude that other genes from the original pool may play minor roles, either individually or in combinations, but end up masked by the effect of major gene KOs. Nonetheless, this subset selection provides a valuable material pool for further research to tackle specific traits (e.g. leaf width, enhanced growth under WD).

While applying the BREEDIT strategy to our case study in maize, we identified a couple of limits to the approach. First, the inability to fully uncouple complex gene interactions. In plant models where transformation and regeneration are efficient, the possibility for massive gene editing grows faster than the capacity to phenotypically analyze the resulting collections of mutants. For complex quantitative traits, large populations of lower-order mutants need to be screened accurately to decipher the complex mechanisms underlying plant development (Liu et al., 2020). To illustrate this, we have developed the following multiplex edited scenario (Supplemental Figure S13). If one would be interested in exhaustively capturing both additive and synergistic gene effects, all the gene KO combinations have to be generated and analyzed. Considering n genes to be targeted, the number of different genetic combinations that have to be produced amounts to 2^n in the case of two-state genes (homozygous wild type or homozygous mutant) (Supplemental Figure S13A) and 3^n if the heterozygous stage has to be considered as well. Given that at least ten replicates per genetic profile (combination) are required to statistically demonstrate a 10% significant difference in FLL3 with enough statistical power (Supplemental Figure S13B), the final amount of plants to be processed increases dramatically as the number of genes in the study grows. Large scale phenotyping/genotyping in field conditions would allow to increase the statistical power to detect combinatorial genes effects that govern agronomic traits, including seed yield.

By applying the BREEDIT strategy on a broad gene set, one could generate a reduced sub-selection of genes of interest underlying a trait and then apply complementary approaches to rule out their contribution to a specific trait of interest in just two generations. One of such approaches is the use of haploid induction (Chaikam et al., 2019; Jacquier et al., 2020), a promising technique to create homozygous mutations, thus removing the need to consider heterozygous material. This could be particularly interesting as a follow up of BREEDIT, because the new gene edits that we observed at T1 were all heterozygous. Another approach is to preselect plants to be phenotyped on the basis of their genetic constitution by predicting gene effects with statistical models in the same fashion as for genomic selection. Such predictions can be combined with the use of non-destructive seed chipping (Mills et al., 2020) to pick specific gene combinations before sowing and therefore reduce the number of plants to be tested. Once the gene space is lowered, the BREEDIT pipeline can be followed again to design validation constructs by engineering a vector containing gRNAs targeting only the genes retained in the selected subset.

In this study, we present the BREEDIT strategy to rapidly generate a large collection of mutants in specific gene families, pathways or networks. We foresee a large potential for BREEDIT combined with existing and more recent breeding approaches, such as marker-assisted breeding, haploid induction, and genomic selection. Effectively implementing the concept of breeding by editing using the BREEDIT pipeline still requires to overcome some practical obstacles, such as the ability to transform and regenerate the plant material, obtain the desired gene KOs and segregate out the original transgene construct. When these conditions are met, applying the BREEDIT pipeline enables to generate many lines with specific combinations of gene KOs able to modify particular traits of interest. These engineered lines could be directly introduced in a hybrid breeding pipeline by crosses to elite material. The impact of favorable allele combinations on complex traits could furthermore be evaluated in different genetic backgrounds and across several generations to assess their heritability. In that perspective, BREEDIT could significantly speed up pre-breeding activities in which pools of diverse materials (wild species, landraces, commercial varieties) are usually screened for promising mutations and phenotypes (Teixeira and Guimarães, 2021) that then have to be transferred into an intermediate set of materials that breeders can use to create new varieties. Introgression of alleles from a divergent pool of materials is often cumbersome because of cross incompatibility, low

seed yield quantity and quality, or persistence of a deleterious linkage drag. Provided that elite materials can be transformed and regenerated, the reverse-genetics approach developed in the BREEDIT pipeline can circumvent the long and tedious step of introgression and save time in the development of new commercial varieties. An additional benefit of BREEDIT could be the generation of large collections of plants mutated in coding or non-coding genome areas using other novel CRISPR technologies such as base editing and promoter bashing to further extend the repertoire of allele variability and phenotypic responses (Vats et al., 2019; Anzalone et al., 2020; Gaillochet et al., 2021).

Materials and methods

Plant material and DNA extraction

The original line used for all transformation procedures was the maize inbred line B104. DNA was extracted following an adapted protocol from Berendzen et al. (2005) coupled with a magnetic beads purification. A piece of 1-2 cm of leaf 1 was ground in 8-strip 2-ml capacity tubes (National Scientific Supply Co). After grinding and centrifugation, the supernatant was mixed with magnetic beads (CleanNA), washed in 80% ethanol and dried for further processing.

Selection of GRGs and curation of gene models

We selected 48 GRGs based on the literature, in house knowledge and orthology searches (see results) in version 4 of the reference maize B73 genome sequence (Jiao et al., 2017). The integrative orthology viewer in PLAZA v4.5 (https://bioinformatics.psb.ugent.be/plaza/versions/plaza_v4_5_monocots/) was used for identification of most orthologous genes, both for finding gene families from other species or for identification of the corresponding maize B104 gene IDs. When required, B104 gene models were manually curated using ORCAE, an online genome annotation resource (https://bioinformatics.psb.ugent.be/orcae/). Comparison of sequences in maize lines B104 and B73 was done by pairwise alignment using Geneious Prime 2020.1.2 (https://www.geneious.com/prime/). Design of the amplicons and gRNAs was performed in Geneious Prime. The maize B73 genome version 4 was used to identify gRNA on-target and off-target sites. gRNAs were selected with specificity score ≥80-85%, no stretch of Ts (>4), without

internal *Bsa*I or *Bbs*I restriction sites, which would interfere gRNA expression and/or vector construction, respectively.

Monitoring CRISPR/Cas9 edits with HiPlex amplicon sequencing

Geneious Prime was used to design primers to amplify the genomic regions surrounding the gRNA cutting sites. A manual selection of two amplicons per gene was done with a size range between 120-150 bp. Each amplicon contained at least two gRNAs separated from either primer by at least 15 bp. The amplicons were selected to target the middle of the coding sequence and to not overlap. The specificity of primers was checked in the maize B73 genome version 4 and only specific primers were retained (Supplemental Table S2). All primers were pooled in a HiPlex amplicon sequencing assay to sequence each locus in each plant simultaneously. HiPlex library preparation was performed by Floodlight Genomics facility (Knoxville, TN, USA) using the MonsterPlex technology. Pilot runs of HiPlex amplicon sequencing were conducted to select the best amplicon per gene (out of the two). The selection was based on amplification efficiency in the HiPlex assay measured as read counts and unambiguous read-reference mapping. Per gene, the overlapping gRNA was selected for cloning into the expression vector. We used SMAP haplotype-window (Schaumont et al., 2022) to trim sequencing reads, identify haplotypes at each locus, and calculate the respective haplotype frequency per locus per sample. SMAP haplotype-window extracts haplotypes from the HiPlex sequencing reads as the entire DNA sequence between the HiPlex primers per locus. Any unique DNA sequence is considered as a haplotype. The total haplotype count is recorded per locus per sample and the relative haplotype frequency per locus per sample is calculated. A haplotype detection threshold of at least 1% relative read depth per locus per sample was set to remove possible spurious haplotypes derived from amplification and/or sequencing artifacts. The nucleotide length difference between the haplotype sequence and the B104 reference sequence (LDR) was used to classify the mutations into three classes: SNPs (LDR = 0 but sequences are different), insertions (LDR > 0, the mutated haplotype is longer than the reference haplotype), and deletions (LDR < 0, the mutated haplotype is shorter than the reference haplotype). We defined haplotypes whose indel length is not a multiple of three nucleotides as haplotype$_{KO}$ because they generate a frame shift in the open reading frame that likely leads to the translation of a wrong amino acid sequence downstream of the mutation, and/or create a premature stop codon, both of which could disrupt the protein function or activity.

Haplotypes with SNPs outside the cutting site and in-frame indels are referred as to Haplotype$_{REF}$ to denote possible minor impact of their mutations on the resulting protein, which may still behave as the reference protein.

Maize is a diploid organism in which each gene has two alleles per nucleus, each derived from one of the two parents. In plant material that stably express CRISPR/Cas9 and gRNAs, continuously driving gene editing, one may expect to observe mosaic tissues, i.e. patches of tissues within an organ that contain different genome sequences due to non-uniform gene editing. Mosaic tissues may occur both in primary transformants and subsequent generations because of the initial and ongoing Cas9 activity, respectively. A single leaf sample used for DNA preparation may therefore contain cells with different gene edits resulting in scoring one individual with more than two alleles. The allele dosage is also affected by mosaicism. Multi-allelism resulting from mosaic tissues blurs the expected 50:50 read depth ratio commonly observed between the two alleles of a diploid organism. In addition, bi-allelism can be observed in non-mosaic tissues, with a plant harboring two indels of a same or different nature (in-frame or out-frame) following a 50:50 read depth ratio. Genotype-to-phenotype statistical associations require discrete genotypic classes (absence/presence, or homozygous wild-type, heterozygous, homozygous mutant). We therefore summed the relative fraction of haplotype$_{KO}$ per locus per sample to quantify how much the locus is affected by mutations leading to a LOF. The resulting aggregation (Σhaplotype$_{KO}$) is discretized in three genotypic classes representing three dosages of haplotype$_{KO}$: LOF$_{0/2}$ (<15% of the read depth per locus per sample contain haplotype$_{KO}$), LOF$_{1/2}$ (between 40% and 60% of the read depth per locus per sample contain haplotype$_{KO}$), and LOF$_{2/2}$ (>85% of the read depth per locus per sample contain haplotype$_{KO}$). Because distinguishing between these three groups is critical to analyze dosage effects associated with a particular trait, any value outside of these three ranges was scored as missing genotype call during the genotype-to-phenotype association analyses.

Construction and cloning of SCRIPT vectors

The gRNA entry vectors were constructed by PCR amplification with Q5 High-Fidelity DNA polymerase (New England Biolabs) of the entire pGG-[B-F]-OsU3-BbsI-ccdB-BbsI-[C-G] plasmids according to the manufacturer's guidelines. The primers contained an extension to insert unique linkers (Torella et al., 2014) between the scaffold and OsU3 promoter (Supplemental

Table S3 and Supplemental Table S4). Two of the five linkers were modified to contain *Not*I restriction sites to facilitate validation of the final expression vectors by restriction digest (Supplemental Figure S1). Gibson assembly was performed with NEBuilder Hifi DNA Assembly Mix (New England Biolabs) to circularize the PCR products into entry vectors using the manufacturer's guidelines. The new entry vectors were confirmed by Sanger sequencing (Mix2Seq service, Eurofins Scientific).

The gRNA construction and Golden Gate assembly into binary vectors was done as previously described (Decaestecker et al., 2019). Briefly, paired gRNA entry vectors were created by PCR amplification (Red Taq DNA Polymerase Master Mix, VWR Life Science or iProof High-Fidelity DNA Polymerase, Bio-Rad Laboratories) on the template plasmid pEN-2xTaU3 with primers containing the 20-nt spacer sequences and *Bbs*I restriction sites. Column-purified PCR products were cloned into the Golden Gate entry vectors via a Golden Gate reaction using *Bbs*I (New England Biolabs). All paired gRNA entry vectors were verified by Sanger sequencing.

Expression vectors (SCRIPT 1-4; Supplemental Figure S1) were constructed by a Golden Gate reaction with *Bsa*I (New England Biolabs) using the paired gRNA entry vectors and a destination vector as previously described (Decaestecker et al., 2019). The destination vector, pGGBb-AG, contains a GreenGate destination module (AG) and a bialaphos-resistance (*bar*) gene driven by the 35S promoter. The expression of each individual gRNA was alternatively driven by either the rice OsU3 promoter or the wheat TaU3 promoter (Xing et al., 2014). The SCRIPT vectors were transformed via heat-shock into *ccd*B-sensitive DH5α *Escherichia coli* cells, grown on LB medium containing 100 µg/mL spectinomycin and extracted with the GeneJET Plasmid Miniprep Kit (Thermo Fisher Scientific). Quality control was performed by restriction digest with *Not*I (Promega). SCRIPTs were transformed into *Agrobacterium tumefaciens* EHA 105 cells by freeze/thaw method and plated on YEB medium with 100 µg/mL rifampicin and 100 µg/mL spectinomycin. The gRNA entry and pGGBb-AG destination vectors can be obtained via https://gatewayvectors.vib.be/.

Generation of EDITOR maize lines

The *zCas9* coding sequence containing a *Zea mays*-codon optimized Cas9 (Xing et al., 2014) was cloned under control of the *ZmUbi1* promoter (pZmUBIL) and NOS terminator in pEN-L4-AG-

R1 (Houbaert et al., 2018) using GreenGate cloning (Lampropoulos et al., 2013). The transcriptional unit was recombined with pEN-L1-linker-L2 and the pHbm42GW7 destination vector (Karimi et al., 2013). The resulting construct pXHb-pZmUBIL-zCas9-NOSt allows to select maize transformants with hygromycin and is referred to as the EDITOR construct.

The EDITOR construct was introduced into the B104 maize line using *Agrobacterium*-mediated transformation of immature embryos (Coussens et al., 2012) and hygromycin as a selection agent. Three independent lines (EDITOR 1 to 3) with a single-locus insertion event were selected and made homozygous for the T-DNA locus by self-crossing. To measure Cas9 protein levels, total proteins from leaf tissue of EDITOR lines were extracted, separated by polyacrylamide gel electrophoresis and blotted on PVDF membrane. For quantification, the blots were stained by incubation with anti-Cas9-HRP primary antibody (Abcam, 1:5000) for 4 h and detected by chemiluminescence. Blots were also Ponceau-stained for protein loading control. EDITOR 1 was crossed with wild-type B104 plants to yield heterozygous immature embryos for a second round of transformation (supertransformation) with each SCRIPT construct separately. Backcrosses render more seeds/embryos compared to self- crosses and also facilitate the removal of Cas9 in the progeny by segregation. For each SCRIPT, at least ten independent T0 supertransformants following BASTA selection were obtained and genotyped by HiPlex amplicon sequencing.

Experimental design and phenotyping

Maize seeds were soaked in water for 24 h and then sown in 0.3-l square pots (7×7×7 cm) using 'potgrond met meststof' (N.V. Van Israel) as substrate. Pots were then arrayed in groups of 24 in 48.0- x 30.5-cm trays, randomized and placed in growth chambers with controlled temperature (24ºC), relative humidity (55%) and a 16:8 photoperiod with controlled light intensity (170-200 µmol/m²/s photosynthetic active radiation provided from a mixture of 50/50 Radium halogen HRI-BT 400W/D Pro Daylight and Philips master son-t pia plus 400-W bulbs).

For WW conditions, plants were grown under a water regime of 2.4 g of water per g of dry potting mix, while for WD assays, this was reduced to 1.1 - 1.4 g of water per g of dry potting mix, which is approximately -100 kPa water potential (Verbraeken et al., 2021). The final leaf length was measured at V3 (FLL3, when the collar of leaf 3 is fully developed) from the crown of the plant to the leaf tip and final leaf width (FLW3) was determined at the middle point of the

691 leaf blade. For biomass, aerial parts of V3 seedlings were harvested and weighed for fresh weight
692 (FW) and then dried in a 60ºC oven to estimate dry weight (DW). Biomass moisture content was
693 calculated on a DW basis as FW-DW/DW.
694
695 **Statistics to detect genotype-to-phenotype associations**
696 Phenotypic datasets were trimmed to remove individuals that scored as under-developed
697 (misshapen or developed less than V3 at the moment of harvest, or over-grown, i.e. that
698 surpassed V3 at the moment of sampling) during the phenotyping trials. Within each population
699 and experiment, one-way ANOVAs were then conducted at the single-gene level to check for
700 differences between the control (EDITOR 1) and mutant groups (either $LOF_{1/2}$ or $LOF_{2/2}$). The
701 minimal size of a mutant group to be considered in statistical analysis was six individuals having
702 both phenotypic and genotypic data. Post-hoc HSD Tukey's tests were then performed to assign
703 each mutant group to a statistical group. Finally, we recorded the number of times a KO (either
704 $LOF_{1/2}$ or $LOF_{2/2}$) of a specific gene was found to be significantly associated with a given trait
705 while leading on average to a >10% increase or decrease compared to the control line (EDITOR
706 1). We compared that count with the number of times sufficient data was available to statistically
707 conclude on a gene KO effect and defined the resulting ratio as the strength of the association.
708
709 **Accession numbers**
710 The entire set of Illumina paired-end read sequences have been deposited at the Sequence Read
711 Archive (DDBJ/ENA/GenBank) under the BioProject accession PRJNA815957.
712
713 **Competing interests**
714 The authors declare that they have no conflicts of interest.
715
716 **Supplemental data**
717 **Supplemental Figure S1.** Map of a SCRIPT construct containing 12 gRNAs.

718 **Supplemental Figure S2.** Location of the 48 growth-related genes over the 10 chromosomes
719 of maize.
720 **Supplemental Figure S3.** Cas9 protein expression levels in three different EDITOR lines.
721 **Supplemental Figure S4.** Comparative summaries of the mutations observed in plants
722 harboring SCRIPT 1 in an EDITOR 1 vs. EDITOR 3 background.
723 **Supplemental Figure S5.** Haplotype overview in T0 material from the four SCRIPTs.
724 **Supplemental Figure S6.** Distribution of the aggregated frequency of haplotypes with out-
725 frame indels (Σ Haplotype KO) in the ingroup samples.
726 **Supplemental Figure S7.** Appearance of new indels in inter-script crosses.
727 **Supplemental Figure S8.** Phenotypes of mutated populations for the four SCRIPTs.
728 **Supplemental Figure S9.** Sterility phenotypes observed in tassels of SCRIPT 1 T0 plants.
729 **Supplemental Figure S10.** Characteristic phenotypes observed in T1 plants of SCRIPT 2
730 under water-deficient conditions.
731 **Supplemental Figure S11.** Characteristic phenotypes observed in T1 plants of SCRIPT 3
732 under water-deficient conditions.
733 **Supplemental Figure S12.** Phenotypes of mutated inter-script populations.
734 **Supplemental Figure S13.** Considerations on numbers for multiplex gene editing
735 experiments.
736 **Supplemental Table S1.** Detailed information of populations used in the phenotyping assays.
737 **Supplemental Table S2.** List of gRNAs and associated primer pairs for edit detection using
738 HiPlex amplicon sequencing.
739 **Supplemental Table S3.** Plasmid overview.
740 **Supplemental Table S4.** Primers used for plasmid building and sequencing.
741

Acknowledgments

The authors would like to thank Lieven Sterck for helping in gene model curation, Mansour Karimi for helping with the cloning of EDITOR constructs, Pan Gong, Reinout Laureyns, and Ji Li for additional help with the selection of the genes.

Funding

This work was supported by the European Research Council (ERC) under the European Union's Horizon 2020 Research and Innovation Programme (H2020/2019-2025) under grant agreement No 833866-BREEDIT.

References

Anzalone AV, Koblan LW, and Liu DR. (2020). Genome editing with CRISPR-Cas nucleases, base editors, transposases and prime editors. Nat. Biotechnol. **38:** 824-844

Ashikari M, Sakakibara H, Lin S, Yamamoto T, Takashi T, Nishimura A, Angeles ER, Qian Q, Kitano H, and Matsuoka M. (2005). Cytokinin oxidase regulates rice grain production. Science **309:** 741-745

Bai M, Yuan J, Kuang H, Gong P, Li S, Zhang Z, Liu B, Sun J, Yang M, Yang L, et al. (2020). Generation of a multiplex mutagenesis population via pooled CRISPR-Cas9 in soya bean. Plant Biotechnol. J. **18:** 721-731

Bartrina I, Otto E, Strnad M, Werner T, and Schmülling T. (2011). Cytokinin regulates the activity of reproductive meristems, flower organ size, ovule formation, and thus seed yield in *Arabidopsis thaliana*. Plant Cell **23:** 69-80

Baute J, Herman D, Coppens F, De Block J, Slabbinck B, Dell'Acqua M, Pè ME, Maere S, Nelissen H, and Inzé D. (2015). Correlation analysis of the transcriptome of growing leaves with mature leaf parameters in a maize RIL population. Genome Biol. **16:** 168

Baute J, Herman D, Coppens F, De Block J, Slabbinck B, Dell'Acqua M, Pè ME, Maere S, Nelissen H, and Inzé D. (2016). Combined large-scale phenotyping and transcriptomics in maize reveals a robust growth regulatory network. Plant Physiol. **170:** 1848-1867

Berendzen K, Searle I, Ravenscroft D, Koncz C, Batschauer A, Coupland G, Somssich IE, and Ülker B. (2005). A rapid and versatile combined DNA/RNA extraction protocol and its application to the analysis of a novel DNA marker set polymorphic between *Arabidopsis thaliana* ecotypes Col-0 and Landsberg *erecta*. Plant Methods **1:** 4

Bhat JA, Yu D, Bohra A, Ganie SA, and Varshney RK. (2021). Features and applications of haplotypes in crop breeding. Commun. Biol. **4:** 1266

Bloch D, Puli MR, Mosquna A, and Yalovsky S. (2019). Abiotic stress modulates root patterning via ABA-regulated microRNA expression in the endodermis initials. Development **146:** dev177097

Borg M, and Berger F. (2015). Chromatin remodelling during male gametophyte development. Plant J. **83:** 177-188

Brás TA, Seixas J, Carvalhais N, and Jägermeyr J. (2021). Severity of drought and heatwave crop losses tripled over the last five decades in Europe. Environ. Res. Lett. **16:** 065012

Cao L, Wang S, Venglat P, Zhao L, Cheng Y, Ye S, Qin Y, Datla R, Zhou Y, and Wang H. (2018). Arabidopsis ICK/KRP cyclin-dependent kinase inhibitors function to ensure the formation of one megaspore mother cell and one functional megaspore per ovule. PLoS Genet. **14:** e1007230

Chaikam V, Molenaar W, Melchinger AE, and Boddupalli PM. (2019). Doubled haploid technology for line development in maize: technical advances and prospects. Theor. Appl. Genet. **132:** 3227-3243

Cheng Y, Cao L, Wang S, Li Y, Shi X, Liu H, Li L, Zhang Z, Fowke LC, Wang H, et al. (2013). Downregulation of multiple CDK inhibitor *ICK/KRP* genes upregulates the E2F pathway and increases cell proliferation, and organ and seed sizes in Arabidopsis. Plant J. **75:** 642-655

Colombo N, and Favret EA. (1996). The effect of gibberellic acid on male fertility in bread wheat. Euphytica **91:** 297-303

Coussens G, Aesaert S, Verelst W, Demeulenaere M, De Buck S, Njuguna E, Inzé D, and Van Lijsebettens M. (2012). *Brachypodium distachyon* promoters as efficient building blocks for transgenic research in maize. J. Exp. Bot. **63:** 4263-4273

Czesnick H, and Lenhard M. (2015). Size control in plants—lessons from leaves and flowers. Cold Spring Harb. Perspect. Biol. **7:** a019190

Decaestecker W, Andrade Buono R, Pfeiffer ML, Vangheluwe N, Jourquin J, Karimi M, Van Isterdael G, Beeckman T, Nowack MK, and Jacobs TB. (2019). CRISPR-TSKO: a technique for efficient mutagenesis in specific cell types, tissues, or organs in Arabidopsis. Plant Cell **31:** 2868-2887

Doll NM, Gilles LM, Gerentes M-F, Richard C, Just J, Fierlej Y, Borrelli VMG, Gendrot G, Ingram GC, Rogowsky PM, et al. (2019). Single and multiple gene knockouts by CRISPR–Cas9 in maize. Plant Cell Rep. **38:** 487-501

Elias F, Muleta D, and Woyessa D. (2016). Effects of phosphate solubilizing fungi on growth and yield of haricot bean (*Phaseolus vulgaris* L.) plants. J. Agric. Sci. **8:** 204-218

Gaillochet C, Develtere W, and Jacobs TB. (2021). CRISPR screens in plants: approaches, guidelines, and future prospects. Plant Cell **33:** 794-813

Gong P, Bontinck M, Demuynck K, De Block J, Gevaert K, Eeckhout D, Persiau G, Aesaert S, Coussens G, Van Lijsebettens M, et al. (2022). SAMBA controls cell division rate during maize development. Plant Physiol. **188:** 411-424

Gong R, Cao H, Zhang J, Xie K, Wang D, and Yu S. (2018). Divergent functions of the GAGA-binding transcription factor family in rice. Plant J. **94:** 32-47

Gonzalez N, Vanhaeren H, and Inzé D. (2012). Leaf size control: complex coordination of cell division and expansion. Trends Plant Sci. **17:** 332-340

Hai NN, Chuong NN, Tu NHC, Kisiala A, Hoang XLT, and Thao NP. (2020). Role and regulation of cytokinins in plant response to drought stress. Plants **9:** 422

He Z, Wu J, Sun X, and Dai M. (2019). The maize clade A PP2C phosphatases play critical roles in multiple abiotic stress responses. Int. J. Mol. Sci. **20:** 3573

Houbaert A, Zhang C, Tiwari M, Wang K, de Marcos Serrano A, Savatin DV, Urs MJ, Zhiponova MK, Gudesblat GE, Vanhoutte I, et al. (2018). POLAR-guided signalling complex assembly and localization drive asymmetric cell division. Nature **563:** 574-578

Huang Y, Wang X, Ge S, and Rao G-Y. (2015). Divergence and adaptive evolution of the gibberellin oxidase genes in plants. BMC Evol. Biol. **15:** 207

Hwang BG, Ryu J, and Lee SJ. (2016). Vulnerability of protoxylem and metaxylem vessels to embolisms and radial refilling in a vascular bundle of maize leaves. Front. Plant Sci. **7:** 941

Ikeda A, Ueguchi-Tanaka M, Sonoda Y, Kitano H, Koshioka M, Futsuhara Y, Matsuoka M, and Yamaguchi J. (2001). *slender* rice, a constitutive gibberellin response mutant, is caused by a null

mutation of the *SLR1* gene, an ortholog of the height-regulating gene *GAI/RGA/RHT/D8*. Plant Cell **13:** 999-1010

Impens L, Jacobs TB, Nelissen H, Inz2 D, and Pauwels L. (2022). Mini-Review: Transgenerational CRISPR/Cas9 gene editing in plants. Frontiers in Genome Editing **4:** 825042

Itoh H, Shimada A, Ueguchi-Tanaka M, Kamiya N, Hasegawa Y, Ashikari M, and Matsuoka M. (2005). Overexpression of a GRAS protein lacking the DELLA domain confers altered gibberellin responses in rice. Plant J. **44:** 669-679

Jacobs TB, Zhang N, Patel D, and Martin GB. (2017). Generation of a collection of mutant tomato lines using pooled CRISPR libraries. Plant Physiol. **174:** 2023-2037

Jacquier NMA, Gilles LM, Pyott DE, Martinant J-P, Rogowsky PM, and Widiez T. (2020). Puzzling out plant reproduction by haploid induction for innovations in plant breeding. Nat. Plants **6:** 610-619

Jiao Y, Peluso P, Shi J, Liang T, Stitzer MC, Wang B, Campbell MS, Stein JC, Wei X, Chin C-S, et al. (2017). Improved maize reference genome with single-molecule technologies. Nature **546:** 524-527

Karimi M, Inzé D, Van Lijsebettens M, and Hilson P. (2013). Gateway vectors for transformation of cereals. Trends Plant Sci. **18:** 1-4

Knott GJ, and Doudna JA. (2018). CRISPR-Cas guides the future of genetic engineering. Science **361:** 866-869

Koyama T, Sato F, and Ohme-Takagi M. (2017). Roles of miR319 and TCP transcription factors in leaf development. Plant Physiol. **175:** 874-885

Lampropoulos A, Sutikovic Z, Wenzl C, Maegele I, Lohmann JU, and Forner J. (2013). GreenGate - A novel, versatile, and efficient cloning system for plant transgenesis. PLoS ONE **8:** e83043

Lan J, and Qin G. (2020). The regulation of CIN-like TCP transcription factors. Int. J. Mol. Sci. **21:** 4498

Lawit SJ, Wych HM, Xu D, Kundu S, and Tomes DT. (2010). Maize DELLA Proteins dwarf plant8 and dwarf plant9 as Modulators of Plant Development. Plant and Cell Physiology **51:** 1854-1868

Li C, Hao M, Wang W, Wang H, Chen F, Chu W, Zhang B, Mei D, Cheng H, and Hu Q. (2018). An efficient CRISPR/Cas9 platform for rapidly generating simultaneous mutagenesis of multiple gene homoeologs in allotetraploid oilseed rape. Front. Plant Sci. **9:** 442

Li J, Wang Z, He G, Ma L, and Deng XW. (2020). CRISPR/Cas9-mediated disruption of *TaNP1* genes results in complete male sterility in bread wheat. J. Genet. Genomics **47:** 263-272

Li N, and Li Y. (2016). Signaling pathways of seed size control in plants. Curr. Opin. Plant Biol. **33:** 23-32

Li W, Herrera-Estrella L, and Tran L-SP. (2016). The yin–yang of cytokinin homeostasis and drought acclimation/adaptation. Trends Plant Sci. **21:** 548-550

Li Y, Shan X, Jiang Z, Zhao L, and Jin F. (2021). Genome-wide identification and expression analysis of the *GA2ox* gene family in maize (*Zea mays* L.) under various abiotic stress conditions. Plant Physiol. Biochem. **166:** 621-633

Liebsch D, and Palatnik JF. (2020). MicroRNA miR396, GRF transcription factors and GIF co-regulators: a conserved plant growth regulatory module with potential for breeding and biotechnology. Curr. Opin. Plant Biol. **53:** 31-42

Liu H-J, Jian L, Xu J, Zhang Q, Zhang M, Jin M, Peng Y, Yan J, Han B, Liu J, et al. (2020). High-throughput CRISPR/Cas9 mutagenesis streamlines trait gene identification in maize. Plant Cell **32:** 1397-1413

Liu L, Gallagher J, Arevalo ED, Chen R, Skopelitis T, Wu Q, Bartlett M, and Jackson D. (2021). Enhancing grain-yield-related traits by CRISPR–Cas9 promoter editing of maize *CLE* genes. Nat. Plants **7:** 287-294

Long SP, Marshall-Colon A, and Zhu X-G. (2015). Meeting the global food demand of the future by engineering crop photosynthesis and yield potential. Cell **161:** 56-66

880 **Lu Y, Ye X, Guo R, Huang J, Wang W, Tang J, Tan L, Zhu J-k, Chu C, and Qian Y.** (2017).
881 Genome-wide targeted mutagenesis in rice using the CRISPR/Cas9 system. Mol. Plant **10:** 1242-
882 1245
883 **McConnell JR, Emery J, Eshed Y, Bao N, Bowman J, and Barton MK.** (2001). Role of *PHABULOSA*
884 and *PHAVOLUTA* in determining radial patterning in shoots. Nature **411:** 709-713
885 **Meng X, Yu H, Zhang Y, Zhuang F, Song X, Gao S, Gao C, and Li J.** (2017). Construction of a
886 genome-wide mutant library in rice using CRISPR/Cas9. Mol. Plant **10:** 1238-1241
887 **Mickelbart MV, Hasegawa PM, and Bailey-Serres J.** (2015). Genetic mechanisms of abiotic stress
888 tolerance that translate to crop yield stability. Nat. Rev. Genet. **16:** 237-251
889 **Miculan M, Nelissen H, Hassen MB, Marroni F, Inzé D, Pè ME, and Dell'Acqua M.** (2021). A
890 forward genetics approach integrating genome-wide association study and expression quantitative
891 trait locus mapping to dissect leaf development in maize (*Zea mays*). Plant J. **107:** 1056-1071
892 **Mills A, Allsman L, Leon S, and Rasmussen C.** (2020). Using seed chipping to genotype maize kernels.
893 Bio-Protocol **101:** e3553
894 **Nelissen H, Rymen B, Jikumaru Y, Demuynck K, Van Lijsebettens M, Kamiya Y, Inzé D, and**
895 **Beemster GTS.** (2012). A local maximum in gibberellin levels regulates maize leaf growth by
896 spatial control of cell division. Curr. Biol. **22:** 1183-1187
897 **Nelissen H, Eeckhout D, Demuynck K, Persiau G, Walton A, van Bel M, Vervoort M, Candaele J,**
898 **De Block J, Aesaert S, et al.** (2015). Dynamic changes in ANGUSTIFOLIA3 complex
899 composition reveal a growth regulatory mechanism in the maize leaf. Plant Cell **27:** 1605-1619
900 **Nuccio ML, Paul M, Bate NJ, Cohn J, and Cutler SR.** (2018). Where are the drought tolerant crops?
901 An assessment of more than two decades of plant biotechnology effort in crop improvement. Plant
902 Sci. **273:** 110-119
903 **Paul BK, Frelat R, Birnholz C, Ebong C, Gahigi A, Groot JCJ, Herrero M, Kagabo DM,**
904 **Notenbaert A, Vanlauwe B, et al.** (2018). Agricultural intensification scenarios, household food
905 availability and greenhouse gas emissions in Rwanda: Ex-ante impacts and trade-offs. Agric. Syst.
906 **163:** 16-26
907 **Poland J, and Rutkoski J.** (2016). Advances and challenges in genomic selection for disease resistance.
908 Annu. Rev. Phytopathol. **54:** 79-98
909 **Qin F, Kodaira K-S, Maruyama K, Mizoi J, Tran L-SP, Fujita Y, Morimoto K, Shinozaki K, and**
910 **Yamaguchi-Shinozaki K.** (2011). *SPINDLY* , a negative regulator of gibberellic acid signaling, is
911 involved in the plant abiotic stress response. Plant Physiol. **157:** 1900-1913
912 **Ramadan M, Alariqi M, Ma Y, Li Y, Liu Z, Zhang R, Jin S, Min L, and Zhang X.** (2021). Efficient
913 CRISPR/Cas9 mediated pooled-sgRNAs assembly accelerates targeting multiple genes related to
914 male sterility in cotton. Plant Methods **17:** 16
915 **Rasheed A, Hao Y, Xia X, Khan A, Xu Y, Varshney RK, and He Z.** (2017). Crop breeding chips and
916 genotyping platforms: progress, challenges, and perspectives. Mol. Plant **10:** 1047-1064
917 **Rida S, Maafi O, López-Malvar A, Revilla P, Riache M, and Djemel A.** (2021). Genetics of
918 germination and seedling traits under drought stress in a MAGIC population of maize. Plants **10:**
919 1786
920 **Rodríguez-Leal D, Lemmon ZH, Man J, Bartlett ME, and Lippman ZB.** (2017). Engineering
921 quantitative trait variation for crop improvement by genome editing. Cell **171:** 470-480.e478
922 **Sarvepalli K, and Nath U.** (2018). CIN-TCP transcription factors: transiting cell proliferation in plants.
923 IUBMB Life **70:** 718-731
924 **Schaumont D, Veeckman E, Van der Jeugt F, Haegeman A, Glabeke Sv, Bawin Y, Lukasiewicz J,**
925 **Blugeon S, Barre P, de la O. Leyva-Pérez M, et al.** (2022). Stack Mapping Anchor Points
926 (SMAP): a versatile suite of tools for read-backed haplotyping. bioRxiv **2022.03.10.483555**
927 **Simmons CR, Lafitte HR, Reimann KS, Brugière N, Roesler K, Albertsen MC, Greene TW, and**
928 **Habben JE.** (2021). Successes and insights of an industry biotech program to enhance maize
929 agronomic traits. Plant Sci. **307:** 110899

Snowdon RJ, Wittkop B, Chen T-W, and Stahl A. (2021). Crop adaptation to climate change as a consequence of long-term breeding. Theor. Appl. Genet. **134:** 1613-1623

Sun X, Cahill J, Van Hautegem T, Feys K, Whipple C, Novák O, Delbare S, Versteele C, Demuynck K, De Block J, et al. (2017). Altered expression of maize *PLASTOCHRON1* enhances biomass and seed yield by extending cell division duration. Nat. Commun. **8:** 14752

Teixeira FF, and Guimarães CT. (2021). Chapter 5 - Maize genetic resources and pre-breeding. In Wild Germplasm for Genetic Improvement in Crop Plants, M.T. Azhar and S.H. Wani, eds (London, United Kingdom: Academic Press, Elsevier), pp. 81-99

Torella JP, Lienert F, Boehm CR, Chen J-H, Way JC, and Silver PA. (2014). Unique nucleotide sequence–guided assembly of repetitive DNA parts for synthetic biology applications. Nat. Protoc. **9:** 2075-2089

Vanhaeren H, Nam Y-J, De Milde L, Chae E, Storme V, Weigel D, Gonzalez N, and Inzé D. (2017). Forever young: the role of ubiquitin receptor DA1 and E3 ligase Big Brother in controlling leaf growth and development. Plant Physiol. **173:** 1269-1282

Vanhaeren H, Gonzalez N, Coppens F, De Milde L, Van Daele T, Vermeersch M, Eloy NB, Storme V, and Inzé D. (2014). Combining growth-promoting genes leads to positive epistasis in *Arabidopsis thaliana*. eLife **3:** e02252

Vats S, Kumawat S, Kumar V, Patil GB, Joshi T, Sonah H, Sharma TR, and Deshmukh R. (2019). Genome editing in plants: exploration of technological advancements and challenges. Cells **8:** 1386

Verbraeken L, Wuyts N, Mertens S, Cannoot B, Maleux K, Demuynck K, De Block J, Merchie J, Dhondt S, Bonaventure G, et al. (2021). Drought affects the rate and duration of organ growth but not inter-organ growth coordination. Plant Physiol. **186:** 1336-1353

Vercruysse J, Baekelandt A, Gonzalez N, and Inzé D. (2020). Molecular networks regulating cell division during Arabidopsis leaf growth. J. Exp. Bot. **71:** 2365-2378

Voorend W, Nelissen H, Vanholme R, De Vliegher A, Van Breusegem F, Boerjan W, Roldán-Ruiz I, Muylle H, and Inzé D. (2016). Overexpression of *GA20-OXIDASE1* impacts plant height, biomass allocation and saccharification efficiency in maize. Plant Biotechnol. J. **14:** 997–1007

Voss-Fels K, and Snowdon RJ. (2016). Understanding and utilizing crop genome diversity via high-resolution genotyping. Plant Biotechnol. J. **14:** 1086-1094

Wang B, Li N, Huang S, Hu J, Wang Q, Tang Y, Yang T, Asmutola P, Wang J, and Yu Q. (2021). Enhanced soluble sugar content in tomato fruit using CRISPR/Cas9-mediated *SlINVINH1* and *SlVPE5* gene editing. PeerJ **9:** e12478

Wang H-Q, Liu P, Zhang J-W, Zhao B, and Ren B-Z. (2020). Endogenous hormones inhibit differentiation of young ears in maize (*Zea mays* L.) under heat stress. Front. Plant Sci. **11:** 533046

Wang H, and Qin F. (2017). Genome-wide association study reveals natural variations contributing to drought resistance in crops. Front. Plant Sci. **8:** 1110

Winkler RG, and Freeling M. (1994). Physiological genetics of the dominant gibberellin-nonresponsive maize dwarfs, *Dwarf8* and *Dwarf9*. Planta **193:** 341-348

Wu L, Zhang D, Xue M, Qian J, He Y, and Wang S. (2014). Overexpression of the maize *GRF10*, an endogenous truncated growth-regulating factor protein, leads to reduction in leaf size and plant height. J. Integr. Plant Biol. **56:** 1053-1063

Xiao Y, Tong H, Yang X, Xu S, Pan Q, Qiao F, Raihan MS, Luo Y, Liu H, Zhang X, et al. (2016). Genome-wide dissection of the maize ear genetic architecture using multiple populations. New Phytol. **210:** 1095-1106

Xing H-L, Dong L, Wang Z-P, Zhang H-Y, Han C-Y, Liu B, Wang X-C, and Chen Q-J. (2014). A CRISPR/Cas9 toolkit for multiplex genome editing in plants. BMC Plant Biol. **14:** 327

Zhang X, and Cai X. (2011). Climate change impacts on global agricultural land availability. Environ. Res. Lett. **6:** 014014

980 **Zhang Y, Malzahn AA, Sretenovic S, and Qi Y.** (2019). The emerging and uncultivated potential of
981 CRISPR technology in plant science. Nat. Plants **5:** 778-794

982 **Table 1. List of the 48 GRGs targeted by different SCRIPTs**

SCRIPT	Position	Gene	Gene family/pathway	B73 V3 gene id	References
1	1	*ZmGa2ox2*	GA2-oxidases	GRMZM2G006964	
1	2	*ZmGa2ox4*	GA2-oxidases	GRMZM2G153359	
1	3	*ZmGa2ox5*	GA2-oxidases	GRMZM2G176963	
1	4	*ZmGa2ox7*	GA2-oxidases	GRMZM2G427618	(Huang et al., 2015; Li et al., 2021)
1	5	*ZmGa2ox8*	GA2-oxidases	GRMZM2G155686	
1	6	*ZmGa2ox9*	GA2-oxidases	GRMZM2G152354	
1	7	*ZmGa2ox13*	GA2-oxidases	GRMZM2G031432	
1	8	*D8*	DELLA/GRAS family	GRMZM2G144744	(Winkler and Freeling, 1994; Lawit et al., 2010)
1	9	*D9*	DELLA/GRAS family	GRMZM2G024973	
1	10	*ZmSLRL1-1*	DELLA/GRAS family	GRMZM5G826526	(Ikeda et al., 2001; Itoh et al., 2005)
1	11	*ZmSLRL2*	DELLA/GRAS family	GRMZM5G874545	
1	12	*ZmSPY*	GA signalling	GRMZM2G357804	(Qin et al., 2011)
2	1	*ZmCKX-2*	cytokinin oxidases	GRMZM2G050997	
2	2	*ZmCKX-3*	cytokinin oxidases	GRMZM2G167220	
2	3	*ZmCKX-4*	cytokinin oxidases	GRMZM5G817173	
2	4	*ZmCKX-4B*	cytokinin oxidases	GRMZM2G024476	
2	5	*ZmCKX-5*	cytokinin oxidases	GRMZM2G325612	
2	6	*ZmCKX-6*	cytokinin oxidases	GRMZM2G404443	(Ashikari et al., 2005; Bartrina et al., 2011)
2	7	*ZmCKX-7*	cytokinin oxidases	GRMZM2G134634	
2	8	*ZmCKX-8*	cytokinin oxidases	GRMZM2G162048	
2	9	*ZmCKX-9*	cytokinin oxidases	GRMZM2G303707	
2	10	*ZmCKX-10*	cytokinin oxidases	GRMZM2G348452	
2	11	*ZmCKX-11*	cytokinin oxidases	GRMZM2G122340	
2	12	*ZmCKX-12*	cytokinin oxidases	GRMZM2G008792	
3	1	*ZmKRP1;1*	ICK/KRP cyclin-dependent kinase	GRMZM2G101613	
3	2	*ZmKRP1;2*	ICK/KRP cyclin-dependent kinase	GRMZM2G084570	
3	3	*ZmKRP1;3*	ICK/KRP cyclin-dependent kinase	GRMZM2G343769	
3	4	*ZmKRP3*	ICK/KRP cyclin-dependent kinase	GRMZM2G154414	(Cheng et al., 2013; Cao et al., 2018)
3	5	*ZmKRP4;2A*	ICK/KRP cyclin-dependent kinase	GRMZM2G037926	
3	6	*ZmKRP4;2B*	ICK/KRP cyclin-dependent kinase	GRMZM2G116885	
3	7	*ZmKRP5;1*	ICK/KRP cyclin-dependent kinase	GRMZM2G358931	
3	8	*ZmKRP5;2*	ICK/KRP cyclin-dependent kinase	GRMZM2G157510	
3	9	*ZmPP2C-A9*	ABA signal transduction	GRMZM2G134628	(He et al., 2019)
3	10	*ZmPP2C-A11*	ABA signal transduction	GRMZM2G159811	
3	11	*ZmHB124B*	Homeobox transcription factor family	GRMZM2G023291	(McConnell et al., 2001)
3	12	*ZmHB124C*	Homeobox transcription factor family	GRMZM2G178102	
4	1	*ZmTCP3*	TCP - CIN clade	GRMZM2G115516	
4	2	*ZmTCP8*	TCP - CIN clade	GRMZM2G020805	
4	3	*ZmTCP9*	TCP - CIN clade	GRMZM2G589470	
4	4	*ZmTCP10*	TCP - CIN clade	GRMZM2G166946	(Koyama et al., 2017; Sarvepalli and Nath, 2018; Lan and Qin, 2020)
4	5	*ZmTCP22*	TCP - CIN clade	GRMZM2G120151	
4	6	*ZmTCP25*	TCP - CIN clade	GRMZM2G035944	
4	7	*ZmTCP42*	TCP - CIN clade	GRMZM2G180568	
4	8	*ZmGRF4*	Growth-regulating factor clade	GRMZM2G004619	
4	9	*ZmGRF10*	Growth-regulating factor clade	GRMZM2G096709	(Nelissen et al., 2012; Voorend et al., 2016; Liebsch and Palatnik, 2020)
4	10	*ZmGRF17*	Growth-regulating factor clade	GRMZM2G124566	
4	11	*ZmPHD8*	SET domain transcription factor	GRMZM2G409224	-
4	12	*ZmBPC6*	GAGA-binding protein	GRMZM2G118690	(Gong et al., 2018)

983

984

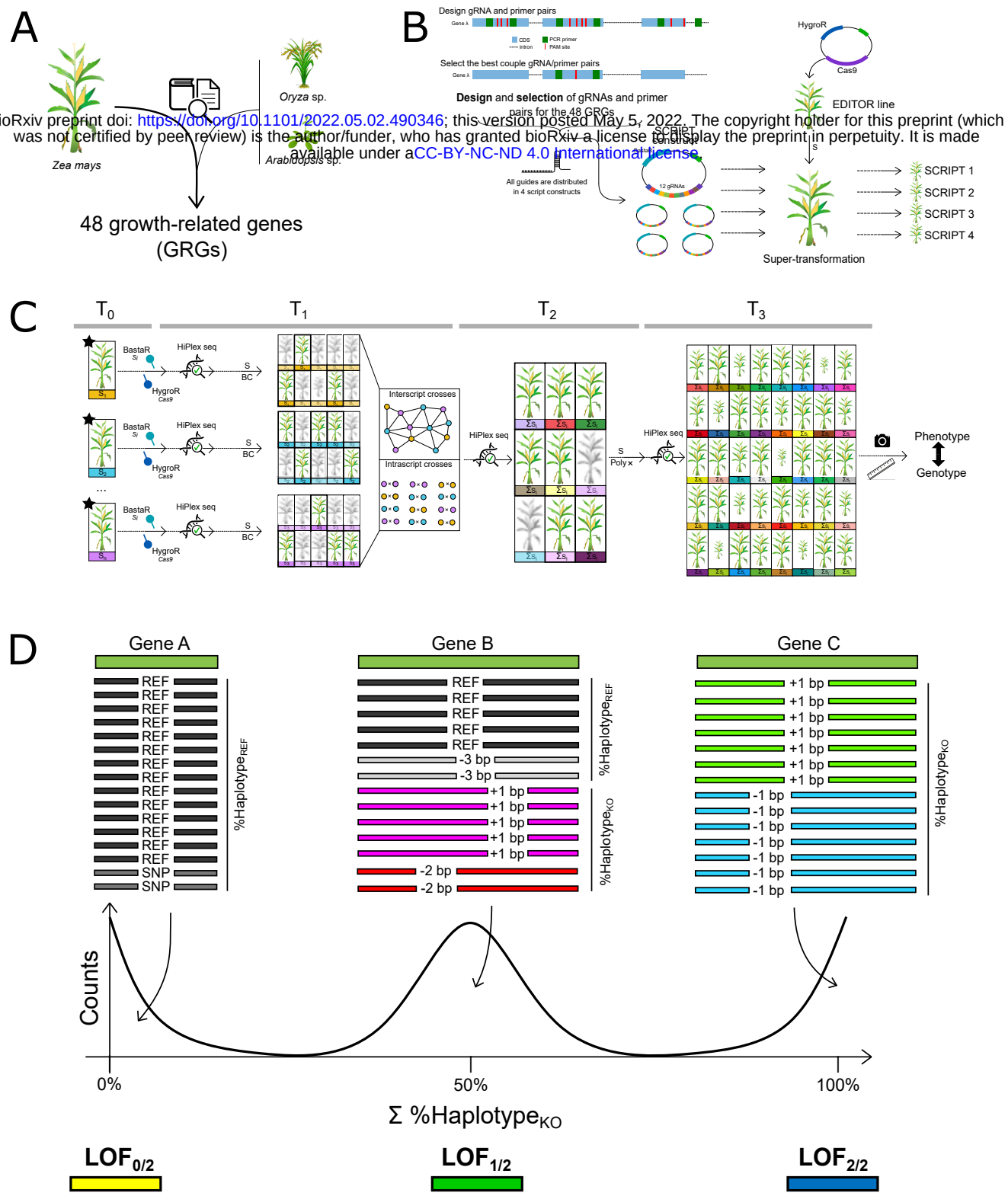

Figure 1. The multiplex gene editing strategy of BREEDIT. **A**. Selection of growth-related genes (GRGs) is based on published and in-house research performed in Arabidopsis, rice or maize **B**. After gene selection, gRNAs with NGG PAM sites are selected for each gene and PCR primer pairs are designed to re-sequence gRNA target sites and flanking regions via HiPlex amplicon sequencing. Per gene, the best set of gRNA and flanking primer pairs is selected. Twelve gRNAs are cloned in multiplex gene editing vectors named "SCRIPTs". Next, the SCRIPT constructs are transformed in a Cas9-expressing maize line named EDITOR. **C**. Vigorous T0 plants containing the SCRIPT (BASTA resistant) and the Cas9 EDITOR construct (hygromycin resistant) are further genotyped using HiPlex amplicon sequencing. Based on the genotypes, plants are selected either for crossing with B104 (BC: backcross), with plants with complementary mutations caused by the same SCRIPT (intra-script crosses) or with plants containing a different SCRIPT and therefore mutations in genes from a different family or pathway (inter-script crosses). These crosses aim at maximizing the mutation landscape and diversity. Finally, self-crosses (S) of lines generate a segregating progeny for high-throughput phenotyping of selected traits, which later can be associated to (combinations of) genes. **D**. From continuous read depth to discrete loss-of-function (LOF) genotypic classes. Sequencing reads are mapped to the B104 reference loci. Two read categories are derived, namely haplotype$_{REF}$ and haplotype$_{KO}$. Haplotype$_{REF}$ corresponds to the aggregated fraction of reads containing only SNPs, in-frame indels or being the reference haplotype. Haplotype$_{KO}$ refers to the aggregated fraction of reads with out-frame indels. A tri-modal distribution is expected for haplotype$_{KO}$, with local maxima around 0%, 50%, 100%, each corresponding to a fraction of the genome being edited at the locus. Haplotype$_{KO}$ is therefore discretized in three gradual classes of LOF: LOF$_{0/2}$ (the genome is not edited with out-frame indels, i.e. 0 chromosome out of 2 in a diploid organism), LOF$_{1/2}$ (half of the genome is edited with out-frame indels, i.e. 1 chromosome out of 2 in a diploid organism), LOF$_{2/2}$ (all the genome is edited with out-frame indels, i.e. 2 chromosomes out of 2 in a diploid organism).

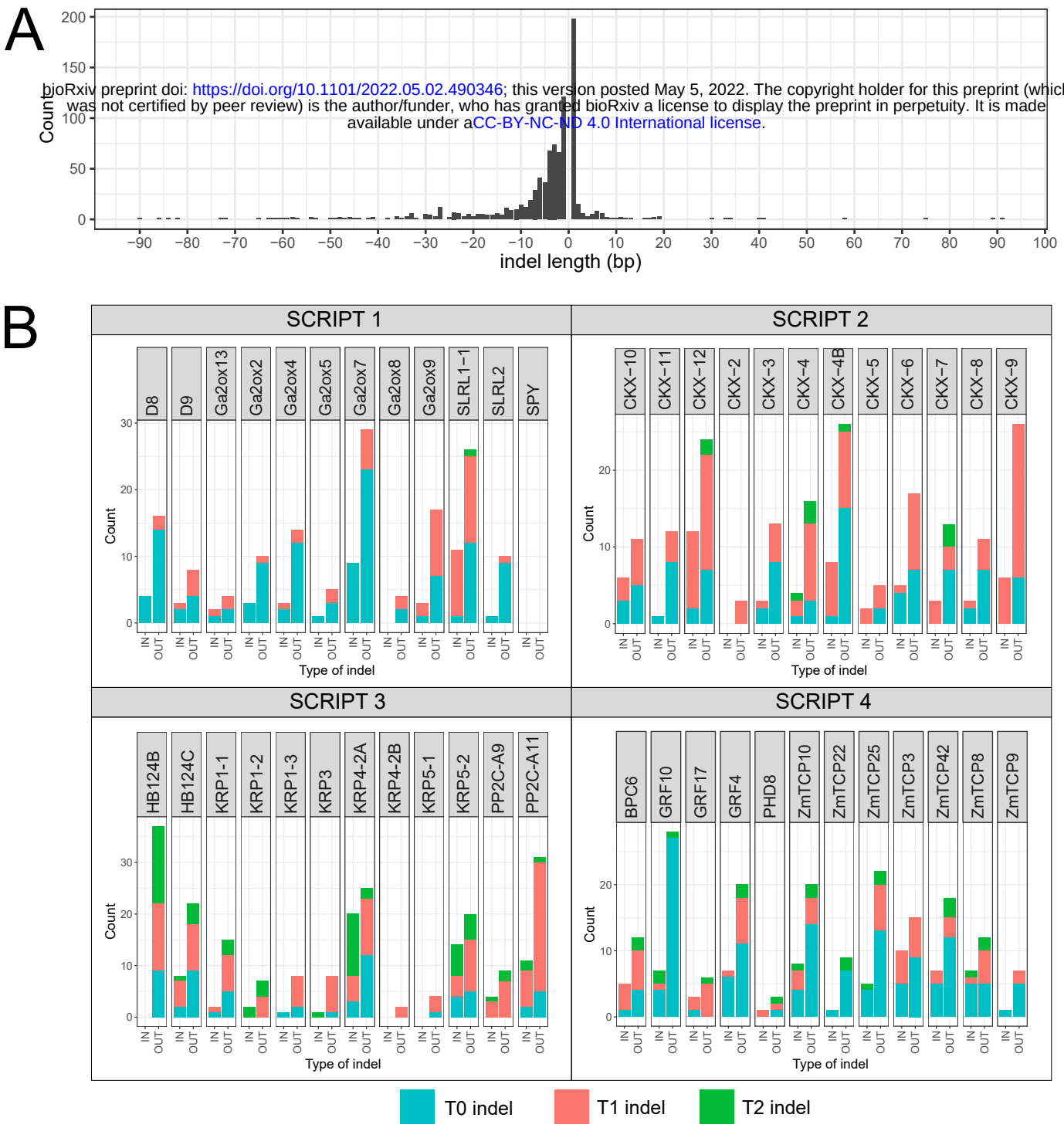

Figure 2. Diversity of mutated haplotypes obtained after CRISPR/Cas9 genome editng. **A**. Distribution of indel length. **B**. Number of different haplotypes with indels observed per gene. Any haplotype with indels with >1% relative frequency in the sequencing reads per locus per sample is included. IN: in-frame indel, OUT: out-frame indel. Blue, red, and green correspond to fractions of indels first observed at T0, T1, and T2, respectively. **C**. Different haplotype combinations in plants can all lead to a gene loss-of-function, either partial ($LOF_{1/2}$) or complete ($LOF_{2/2}$). Each colored horizontal stacked bar corresponds to a different $haplotype_{KO}$. Bar length is proportional to the fraction of sequencing reads per locus containing the $haplotype_{KO}$. The black fraction corresponds to the aggregation of alleles assigned to the wild-type haplotype ($haplotype_{REF}$). For an overview of the different $haplotype_{KO}$ found in T0 plants harboring the different SCRIPTs, see Supplemental Figure S5.

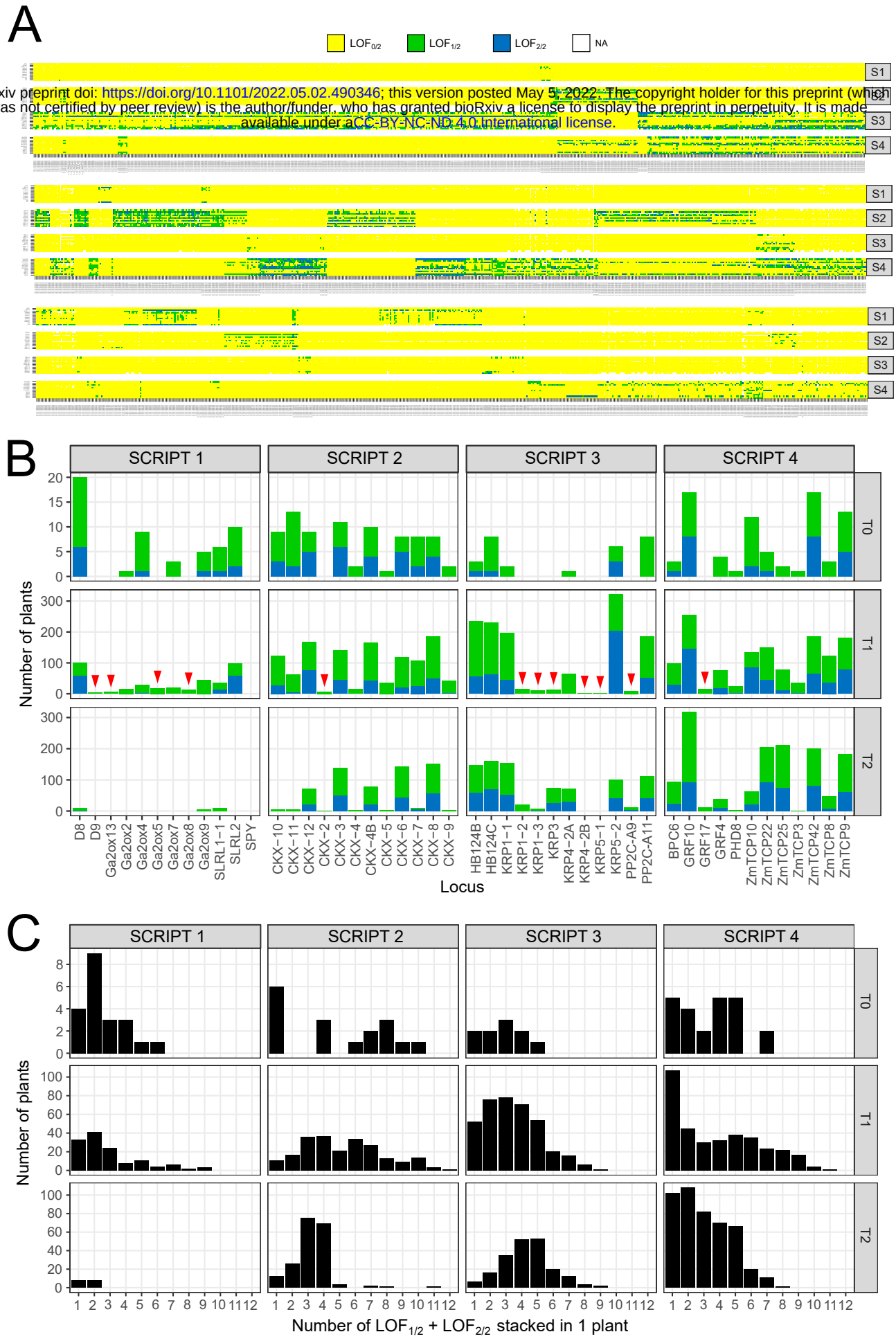

Figure 3. Distribution of LOF in genes across the entire set of samples. Only haplotype$_{KO}$ were considered for genotype calling. The fractions of reads containing haplotype$_{KO}$ were summed per sample per locus. **A**. Overview of the classes LOF$_{0/2}$, LOF$_{1/2}$, or LOF$_{2/2}$ obtained in the entire sample set for the four SCRIPTS (S1-S4). Samples are on the x-axis and distributed over three rows. **B.** Distributions of LOF$_{1/2}$ (green) and LOF$_{2/2}$ (blue) across the four SCRIPTs throughout generations. The top, middle, and bottom panels show T0, T1, and T2 plants, respectively. Red triangles indicate new LOF that appeared at T1. **C**. Stacking LOF at multiple genes within plants.

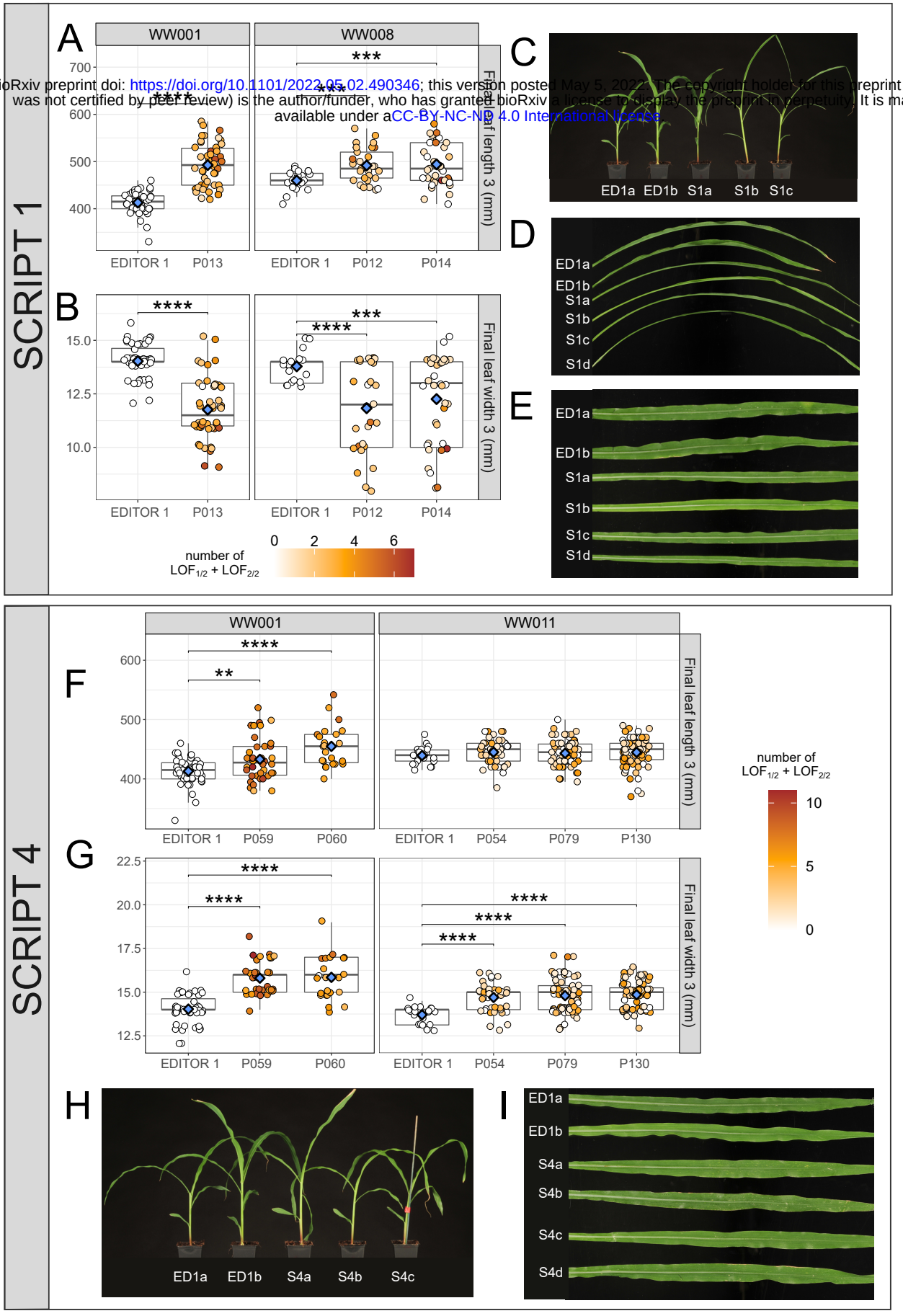

Figure 4. Phenotypes observed in multiple gene-edited populations of SCRIPT 1 and SCRIPT 4. A-B, F-G. Measurements of final length of leaf 3 (FLL3) (A, F) and final leaf width (FLW3) (B, G) of gene-edited SCRIPT 1 (A, B) and SCRIPT 4 (F, G) individuals compared with the EDITOR 1 background control. For each SCRIPT, data corresponds to independent multiple gene-edited populations assayed on two different independent experiments under WW conditions. On the distributions, each dot represents one individual and is colored according to the amount of partial ($LOF_{1/2}$) and complete ($LOF_{2/2}$) LOF observed in that individual. The more orange, the higher the LOF in the individual. Pairwise Student's t-test were conducted between EDITOR 1 and mutated populations. Significant differences are displayed with p-values summarized as follow: **= p<0.01, *** = p<1e-3, **** = p <1e-4. Blue diamonds indicate the mean of each distribution. C-D, H-I. Pictures of general plant architecture (C for SCRIPT 1 and H for SCRIPT 4) and final leaf 3 (D for SCRIPT 1 and I for SCRIPT 4) compared with the EDITOR 1 (ED1) background.

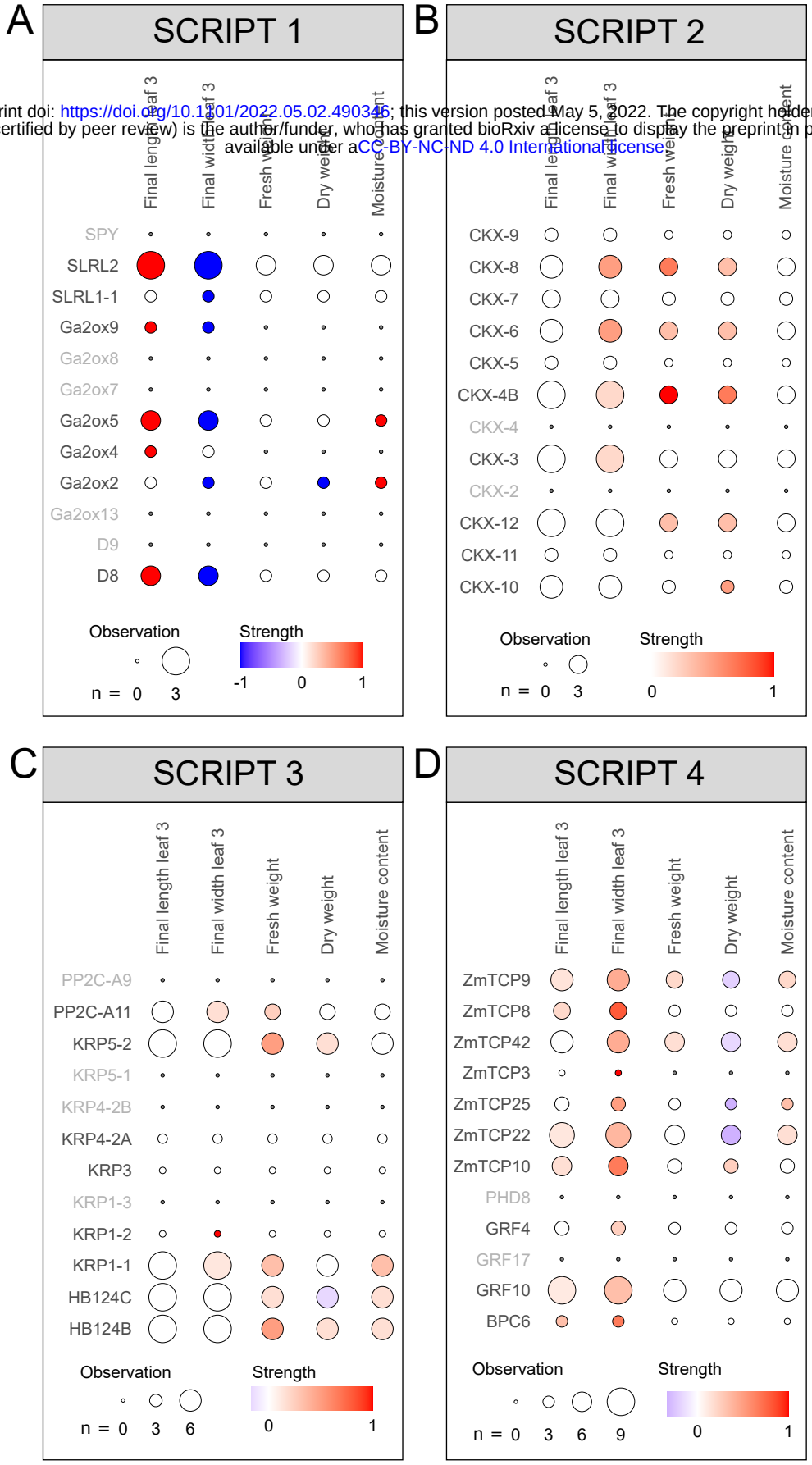

Figure 5. Aggregated association analysis of single-gene LOF and traits. Summaries of single-gene associations to traits are represented for SCRIPT 1 (A), SCRIPT 2 (B), SCRIPT 3 (C), and SCRIPT 4 (D). Single-gene associations were performed per population, in each phenotypic experiment and for all measured traits. Results are summarized per gene, per trait with two indices. 1) Observation: the number of time a given gene has been observed in a situation with sufficient genotypic and phenotypic data across populations and experiments. An observation with sufficient data corresponds to a situation where a gene displays at least one LOF group between $LOF_{1/2}$ and $LOF_{2/2}$ represented by at least six individuals with phenotypic information for a specific trait. In such cases, the mean phenotypic value of each genotypic group could be statistically compared to the mean phenotypic value of the EDITOR 1 control. 2) Strength: for each gene, we calculated the weighted sum of observations in which the genotypic group with the highest mean phenotypic value is above (weight: +1) or below (weight: -1) 10% the mean phenotypic value of EDITOR 1. The resulting sum was divided by the total number of observations (n). Associations displaying highest strength, either positive or negative, along with a large total number of observations indicate strong evidence for a gene effect on the trait.

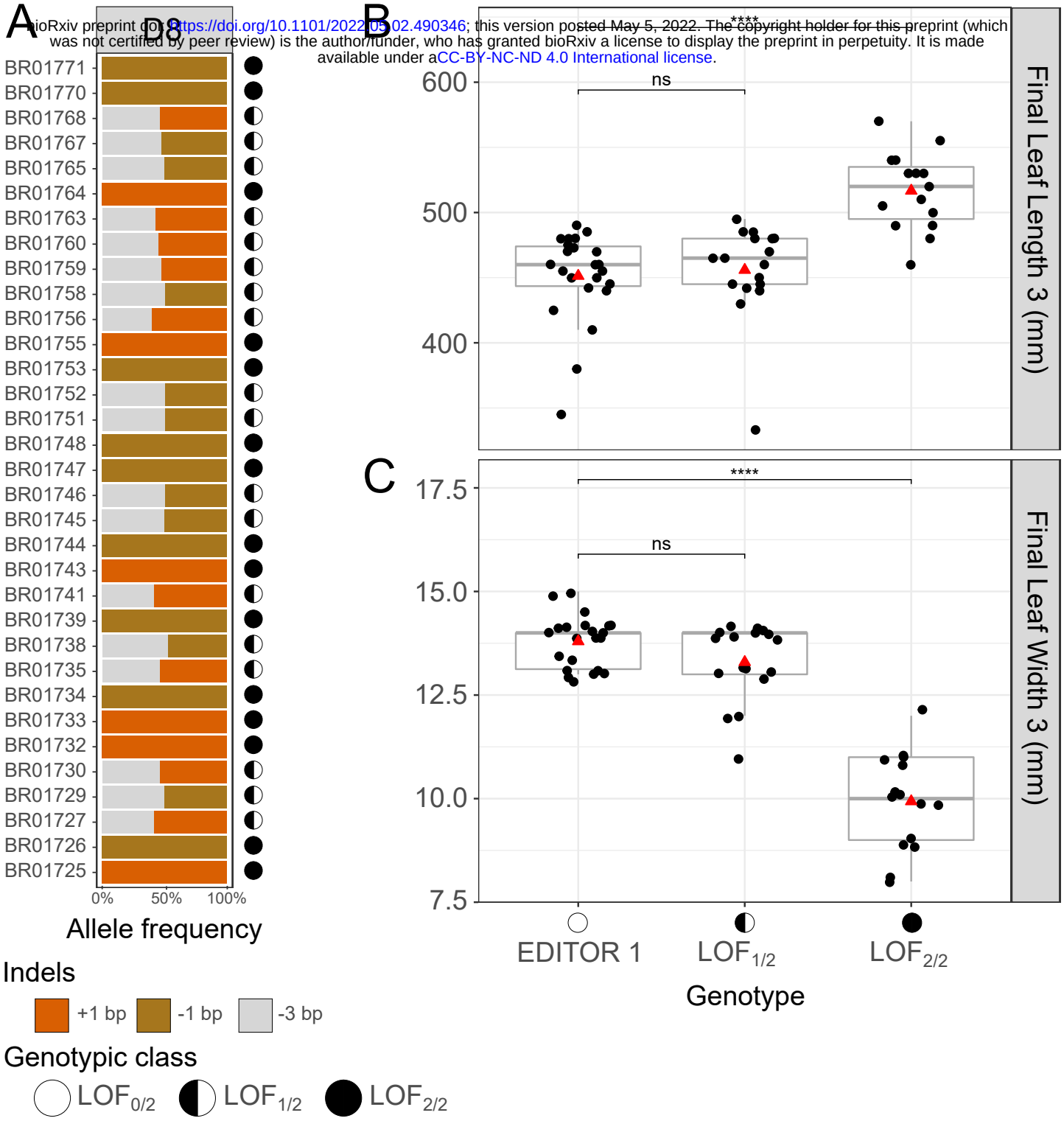

Figure 6. LOF dosages in *D8* and leaf shape parameters. **A**. Haplotype profiles at gene *D8* of T1 segregants from population P012. Three haplotypes were detected, with two containing out-frame indels (-1 bp, brown and +1 bp, orange) and one containing an in-frame (-3 bp, gray) deletion. This results in a collection of plants with *D8* either partially ($LOF_{1/2}$) or completely ($LOF_{2/2}$) knocked out. The resulting two classes of LOF dosages are compared to EDITOR 1 for final leaf length 3 (**B**) and final leaf width 3 (**C**). Significant differences (pairwise Student's *t*-test) are displayed with p-values summarized as follow: *** = p<1e-3, ns: not-significant. Red triangles indicate the mean of each distribution.

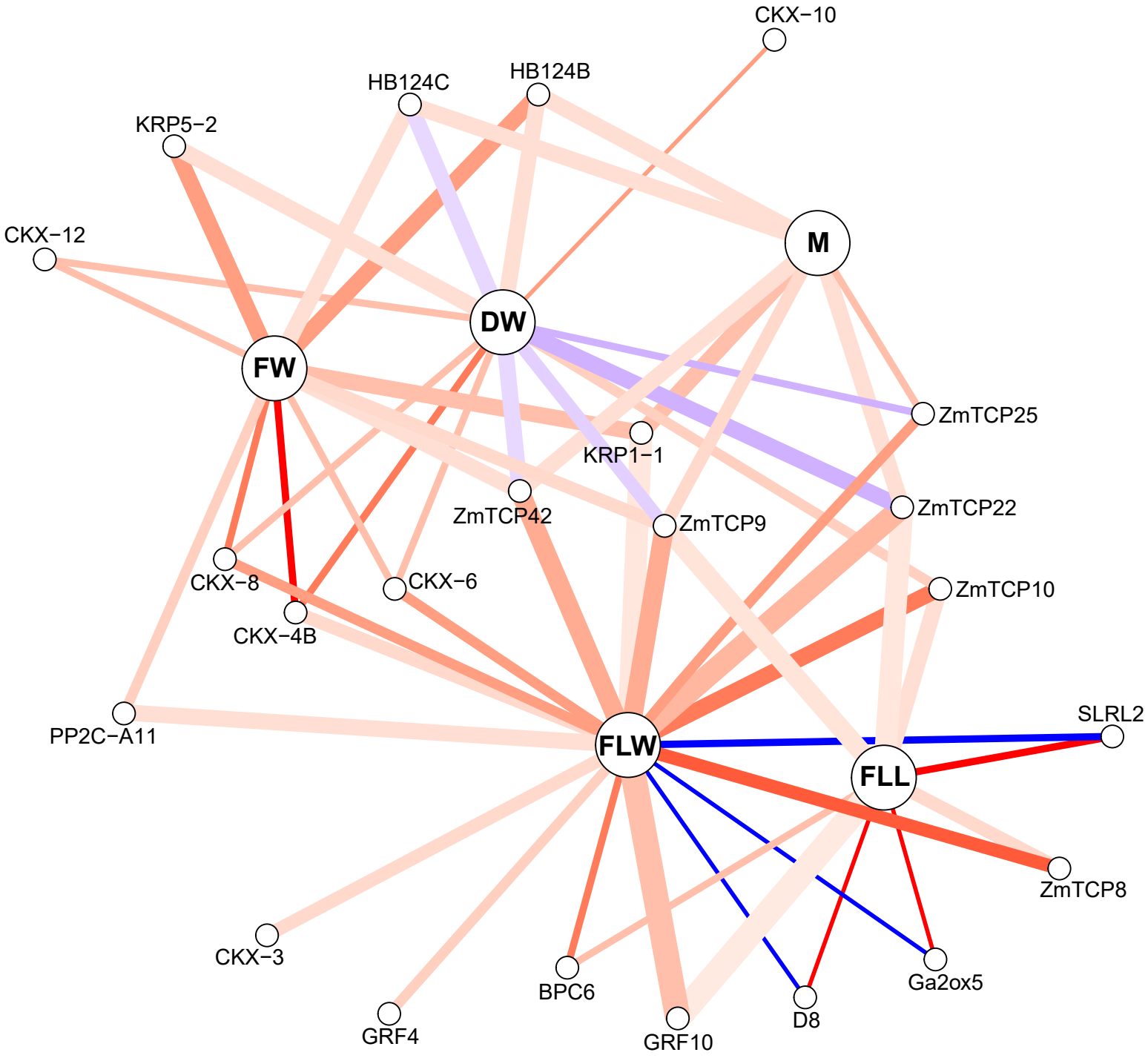

Figure 7. Network representation of single-gene effects on growth-related traits. Traits are displayed in bold (FLL: final leaf length; FLW: final leaf width; FW: fresh weight; DW: dry weight; M: moisture content). Genes at least associated once with a trait are displayed. Lines indicate connections between genes and traits. Line width is proportional to the number of times the underlying dataset to detect a gene knockout-trait association in different experiments and/or populations contained sufficient data for statistics (i.e., minimum one LOF class between $LOF_{1/2}$ and $LOF_{2/2}$ with at least six individuals with phenotypic information). Line color represents the weighted fraction of gene KO-trait associations that significantly outperformed by 10% the EDITOR 1 control (ANOVA test; p<5%), either positively (weight: +1, more red) or negatively (weight: -1, more blue), over the number of times a gene KO-trait association could have been observed because of sufficient data points.

ID population	Scripts	Generation	Type	Total edited loci	Fixed loci	Experiment
P012	S1	T1	Self	9/12	1	WW08
P013	S1	T1	Intrascript	11/12	2	WW01
P014	S1	T1	Self	9/12	1	WW08
P019	S2	T1	Self	10/12	2	WW01, WD03
P108	S2	T1	Intrascript	11/12	0	WW01, WD05
P032	S3	T1	Self	6/12	0	WW1
P033	S3	T1	Self	7/12	1	WW1,WD07
P034	S3	T1	Intrascript	10/12	1	WD07
P030	S3	T1	Self	5/12	0	WD07
P059	S4	T1	Intrascript	12/12	5	WW01
P060	S4	T1	Self	9/12	5	WW01
P054	S4	T1	Self	9/12	0	WW11
P079	S4	T1	Self	10/12	0	WW11
P130	S4	T2	Self	11/12	0	WW11
P148	S2 + S4	T2	Interscript	7/24	0	WD09
P152	S2 + S4	T2	Interscript	8/24	0	WD09
P157	S3 + S4	T2	Interscript	16/24	0	WD06
P158	S3 + S4	T2	Interscript	16/24	0	WD06

Supplemental Table 1: Detailed information of populations used in the phenotyping assays. The number of loci edited correspond to segregating or fixed loci with an aggregated ratio of indels of 40% in at least 3 plants in the population.

Script	Position	Gene	gRNA	Amplicon primer Fw	Amplicon Primer Rv
1	1	*ZmGa2ox2*	TATATGCAGGGACGTGGTGCAGG	GGCCTAAAAACCAGAGCTGC	CCTCGTCGTGGCCCAGAAG
1	2	*ZmGa2ox4*	GGCGCGATGTCAAAGCTGGCCGG	ACATATCGGTGCAGCAGGG	GTCTCGTCGCACCCCTCC
1	3	*ZmGa2ox5*	CGGACGGGTCAGCCGGCACCTGG	AACGACGTGGACGGCCTG	ATCTCACCGACCTGAAGGGC
1	4	*ZmGa2ox7*	TGACGGGACAGGGGAGGCCTTGG	CGACATGGGGTGGCTCGA	TTCGCTGACACTGCATGCAT
1	5	*ZmGa2ox8*	CGACGAGATCTTCACGGTGTTGG	GGTACGGCAGCAAGAGCATC	CGAAGACGAGGCAACAACAA
1	6	*ZmGa2ox9*	CCGCGCCGGCCGGGCCGTTACGG	CATTATTGCCCTGCGCCG	GACTCAGGAGGCAAGCGAAG
1	7	*ZmGa2ox13*	AGGCAGGGGTAGTTCAGCGCCGG	GCGGACAGCGACTGCATG	GGAGCACCGAGATGATCTGC
1	8	*D8*	TCGAGGAGGGAGCTGTCCGGTGG	GCAAGGTCGCCGCCTACT	GTAGGGGCAGGACTCGTAGA
1	9	*D9*	GGAGGGAGCCGTCCGGTGCCGGG	GCAAGGTCGCCGCCTACT	GTAGGGGCAGGACTCGTAGA
1	10	*ZmSLRL1-1*	ACGGCGGCCCAATGCCCGTGAGG	CTGATCCAGGCCCTCGCG	GGAGAAGTGGACGCGCAC
1	11	*ZmSLRL2*	GTACACCTCTGTGAGTGAGTCGG	ATGCCCTCTTCCACTATGCG	TCGCCGCAGACAATGTCAAA
1	12	*ZmSPY*	GATAACTCCCATGTTGCAATAGG	TGTTACGAGAAAGCTGCACT	AGCATACCTCTCGTAGCAGA
2	1	*ZmCKX-2*	ATAGCACTCTTCCATCTGACTGG	CAGGACAGGCATCCTCAACA	CCATGGTATCAGTGTCGCCA
2	2	*ZmCKX-3*	TGAGACGCTCAAGCACGGTCTGG	CCCGGAGGAGAGCTCTGGATCA	GACATTGCTGACCTGCGGTCCG
2	3	*ZmCKX-4*	CTTGAGCGAGGTGAGCTTCACGG	GGGCCTCATCAACAACTGGA	CTGCGGTTTCGTCGTCGTAG
2	4	*ZmCKX-4B*	TGTTGTGGCTGTTACCCTTTGGG	AACCCGGACCTATTCTTCGG	GGGAGAGACAGGAGGGAGAG
2	5	*ZmCKX-5*	TTCCTGGACCGCGTGAGCGCCGG	GACGTGATGCTGCGTGAG	GAGGTTGAGCCACGGGTG
2	6	*ZmCKX-6*	GTTCATCTGAACCGGGTCAGGATGG	CGTGGAGGCCATCTCGAG	GTGCACCTCCTCCCACATC
2	7	*ZmCKX-7*	GTTCATCTGAACCGGGTCAGGATGG	GAACAATGCAGGCACAGGTG	CTCAAGCCGGATCCGTGC
2	8	*ZmCKX-8*	GAACTCGGACCTGTTCATGGCGG	GAACAATGCAGGCACAGGTG	CTCAAGCCGGATCCGTGC
2	9	*ZmCKX-9*	CACCCAATGCTGCGTAGAACAGG	TGTGTGATCGAGCTGTGTTT	GTTCAAGCGCGATCCGAG
2	10	*ZmCKX-10*	AGGCCCCGCACGTGCTTGAGCGG	CGTTGGTTATGGTTCGTGCG	TCCTCCTCCACCCGGTTC
2	11	*ZmCKX-11*	TCCTCTGCAGGTTGTGGACCTGG	GAAGGGCCATTGTTGACGAC	CCGCACCCAGTTGAGGAAAT
2	12	*ZmCKX-12*	TTGGGCGGAGCAACTTGCAGCGG	TTCTTCGCCGTACTTGGTGG	ACCAGCTAGAGAGGAAGCAG
3	1	*ZmKRP1;1*	CTCGCGGTCTGGGCCGCTCCCGG	CTACGACGTAACAGGCTGGC	TTCAGCAGGAATCGCGAGAC
3	2	*ZmKRP1;2*	TGTCGTCACCGCGAGCAACTCGG	ATTGTGCGGGCTCTAACTCT	ACGGTGGGAGGCATAATTCA
3	3	*ZmKRP1;3*	CGCAGAAGCTGTGCTCGCGACGG	CAACGTGGGGAGGACGAC	GTGTTCCCAGTCACTGCCG
3	4	*ZmKRP3*	CTTACGCCTCTGCGAATCGCCGG	GGAAACCGAGATAGAGGCCT	CACCACGCCAACCCAACT
3	5	*ZmKRP4;2A*	CTCCTCACGGACGCCACCTGCGG	GCGAGTACCTGGAGCTAAGG	CATGTTCTCCCCGTACGACG
3	6	*ZmKRP4;2B*	CCCGACCTCCTCGTGGTCGCCGG	GCGAGTACCTGGAGCTAAGG	CATGTTCTCCCCGTACGACG
3	7	*ZmKRP5;1*	CCGCACGCTCGCGCTGCAGAGGG	GTGGCCGTCATGGAGGTC	TCCTGAGCTCGAGGTACTGT
3	8	*ZmKRP5;2*	CGGTATGAACCGGCAGCTCGGGG	CCCAGAGATGATAAGCACCCC	GAACTCCTCCATCTCGAGCG
3	9	*ZmPP2C-A9*	GGCTCGCCCATGCACTTCTTCGG	CTCGCTCCATCCGGACTTG	GACTAGCTGGAGATTGGCGG
3	10	*ZmPP2C-A11*	GACACTCGTGCCAGAACCTGTGG	GGAGGTGGTGAAGAAGCAGG	GCCCGTGAATCTCCACAGTT
3	11	*ZmHB124B*	CATGGAGGATATCCACGCACCGG	ACTAGTCCATAGGTCGCGGA	ACCTGCATGTAGATAAGCTCGA
3	12	*ZmHB124C*	AGGTCATTGACTCAGTCCACTGG	TTTTGCTTGATCATTATATTTGATGCA	GGAAGCACCTCAGCTCTGAT
4	1	*ZmTCP3*	AGGCGCGCACGGGCTGTCGACGG	ATCAGCAGCCCAACGTCTC	CCGAACGGAGGCGCATTG
4	2	*ZmTCP8*	CAGCACTTCGGCTTGGCCAGTGG	GCTCCTCACCTCGGCAAC	GCAAGAACGAGAACTGCGTC
4	3	*ZmTCP9*	CAGCTCCTGGCTGTGTCCGCCGG	CAGTCGTCGACCATGGGG	GACCGGTGGTGGAACATGG
4	4	*ZmTCP10*	TGCCCAACCATGAGGTCCTGCGG	TCAACCAGCCTAGCAAGGTC	TTCTCGTCGTGCACCATCAG
4	5	*ZmTCP22*	CCAGTTCCCGCCGCAAGGGCAGG	GAGCAAGGTGGTGGACTGG	CTGCAACGTTGGCAAAGGG
4	6	*ZmTCP25*	GTACCGGTCCAAGACTCGCCGGG	AATTCCATCCGCCTCGTCAA	GAGATGAGAAGGGCGAGTGG
4	7	*ZmTCP42*	CTCGAAGGATATGGCCGACGCGG	CGCCAACAACAGCAGCAAG	GGCTGCTCCTGAAGGAAGG
4	8	*ZmGRF4*	CATCCGTCCCTGACGGTGCTGGG	CTGGTTACAGCTGCAGCAAC	TGATAAACCCGGGACTGCTG
4	9	*ZmGRF10*	GGACCTCCGGATCCTCGACCAGG	GACAAGGCGGATCGAGAGG	GAGAGAGTCAGCCAGAACGG
4	10	*ZmGRF17*	TTCTGTCCTGTTCGCAGGAGAGG	CTGATCGCTCTGTGTTTGGC	GGACACATCCGCGTCTCG
4	11	*ZmPHD8*	CACTGGACATATGAACAAACCGG	AGTGGAACAGGAAAAATGGGGT	TCTGTCCTGTTTACTAGCTTCTCA
4	12	*ZmBPC6*	TTCTTTGTTCCATTGAGAGGAGG	CCCTAGCTGCACTCGAACTC	GCGGGGATGTTTGGACATGA

Supplemental Table 2: List of gRNAs and associated primer pairs for edit detection using HiPlex amplicon sequencing.

Full name	type	Cloning sites	Bacterial Selection	Plant Selection
pGG-A-OsU3-BbsI-ccdB-BbsI-B	Entry vector	A-B	Ampicilin	
pGG-B-OsU3-BbsI-ccdB-BbsI-C	Entry vector	B-C	Ampicilin	
pGG-C-OsU3-BbsI-ccdB-BbsI-D	Entry vector	C-D	Ampicilin	
pGG-D-OsU3-BbsI-ccdB-BbsI-E	Entry vector	D-E	Ampicilin	
pGG-E-OsU3-BbsI-ccdB-BbsI-F	Entry vector	E-F	Ampicilin	
pGG-F-OsU3-BbsI-ccdB-BbsI-G	Entry vector	F-G	Ampicilin	
pGG-B-U1-OsU3-BbsI-ccdB-BbsI-C	Entry vector with U-linker	B-C	Ampicilin	
pGG-C-U2-OsU3-BbsI-ccdB-BbsI-D	Entry vector with U-linker	C-D	Ampicilin	
pGG-D-U3-OsU3-BbsI-ccdB-BbsI-E	Entry vector with U-linker	D-E	Ampicilin	
pGG-E-U4-OsU3-BbsI-ccdB-BbsI-F	Entry vector with U-linker	E-F	Ampicilin	
pGG-F-U5-OsU3-BbsI-ccdB-BbsI-G	Entry vector with U-linker	F-G	Ampicilin	
pEN-2xTaU3	PCR template		Kanamycin	
pGG-A-Script1-entry1-B	Paired gRNA entry vector	A-B	Ampicilin	
pGG-B-Script1-entry2-C	Paired gRNA entry vector	B-C	Ampicilin	
pGG-C-Script1-entry3-D	Paired gRNA entry vector	C-D	Ampicilin	
pGG-D-Script1-entry4-E	Paired gRNA entry vector	D-E	Ampicilin	
pGG-E-Script1-entry5-F	Paired gRNA entry vector	E-F	Ampicilin	
pGG-F-Script1-entry6-G	Paired gRNA entry vector	F-G	Ampicilin	
pGG-A-Script2-entry1-B	Paired gRNA entry vector	A-B	Ampicilin	
pGG-B-Script2-entry2-C	Paired gRNA entry vector	B-C	Ampicilin	
pGG-C-Script2-entry3-D	Paired gRNA entry vector	C-D	Ampicilin	
pGG-D-Script2-entry4-E	Paired gRNA entry vector	D-E	Ampicilin	
pGG-E-Script2-entry5-F	Paired gRNA entry vector	E-F	Ampicilin	
pGG-F-Script2-entry6-G	Paired gRNA entry vector	F-G	Ampicilin	
pGG-A-Script2-entry1-B	Paired gRNA entry vector	A-B	Ampicilin	
pGG-B-Script3-entry2-C	Paired gRNA entry vector	B-C	Ampicilin	
pGG-C-Script3-entry3-D	Paired gRNA entry vector	C-D	Ampicilin	
pGG-D-Script3-entry4-E	Paired gRNA entry vector	D-E	Ampicilin	
pGG-E-Script3-entry5-F	Paired gRNA entry vector	E-F	Ampicilin	
pGG-F-Script3-entry6-G	Paired gRNA entry vector	F-G	Ampicilin	
pGG-A-Script4-entry1-B	Paired gRNA entry vector	A-B	Ampicilin	
pGG-B-Script4-entry2-C	Paired gRNA entry vector	B-C	Ampicilin	
pGG-C-Script4-entry3-D	Paired gRNA entry vector	C-D	Ampicilin	
pGG-D-Script4-entry4-E	Paired gRNA entry vector	D-E	Ampicilin	
pGG-E-Script4-entry5-F	Paired gRNA entry vector	E-F	Ampicilin	
pGG-F-Script4-entry6-G	Paired gRNA entry vector	F-G	Ampicilin	
pGG-A-Script5-entry1-B	Paired gRNA entry vector	A-B	Ampicilin	
pGG-B-Script5-entry2-C	Paired gRNA entry vector	B-C	Ampicilin	
pGG-C-Script5-entry3-D	Paired gRNA entry vector	C-D	Ampicilin	
pGG-D-Script5-entry4-E	Paired gRNA entry vector	D-E	Ampicilin	
pGG-E-Script5-entry5-F	Paired gRNA entry vector	E-F	Ampicilin	
pGG-F-Script5-entry6-G	Paired gRNA entry vector	F-G	Ampicilin	
pGGBb-AG	Destination vector	A-G	Spectinomycin	Bar
pGG-AG-Script1	Expression vector	A-G	Spectinomycin	Bar
pGG-AG-Script2	Expression vector	A-G	Spectinomycin	Bar
pGG-AG-Script3	Expression vector	A-G	Spectinomycin	Bar
pGG-AG-Script4	Expression vector	A-G	Spectinomycin	Bar
pGG-AG-Script5	Expression vector	A-G	Spectinomycin	Bar

Supplemental Table 3: Plasmid overview.

Oligo number	Name	Sequence	Description	Template PCR	Method
2110	F_U1	ATCCATTCTCAGGCTGTCTCGTCTCGTCTCAGTAATTCATCCAGGTCACC	Cloning pGG-B-U1-OsU3-BbsI-ccdB-BbsI-C	pGG-B-OsU3-BbsI-ccdB-BbsI-C	Gibson assembly
2111	R_U1	GAGACAGCCTGAGAATGGATGCGAGTAATGTGTTTGAGACCAAGCTTCAC	Cloning pGG-B-U1-OsU3-BbsI-ccdB-BbsI-C	pGG-B-OsU3-BbsI-ccdB-BbsI-C	Gibson assembly
2112	F_U2	CGTAGACGCGGCCGCACGCAGAATCCAAGCAGTAATTCATCCAGGTCACC	Cloning pGG-C-U2-OsU3-BbsI-ccdB-BbsI-D	pGG-C-OsU3-BbsI-ccdB-BbsI-D	Gibson assembly
2113	R_U2	TGCGTGCGGCCGCGTCTACGAACTCCCAGCAGCCTGAGACCAAGCTTCAC	Cloning pGG-C-U2-OsU3-BbsI-ccdB-BbsI-D	pGG-C-OsU3-BbsI-ccdB-BbsI-D	Gibson assembly
2114	F_U3	TCCTCAATCGCACTGGAAACATCAAGGTCGAGTAATTCATCCAGGTCACC	Cloning pGG-D-U3-OsU3-BbsI-ccdB-BbsI-E	pGG-D-OsU3-BbsI-ccdB-BbsI-E	Gibson assembly
2115	R_U3	GTTTCCAGTGCGATTGAGGACCTTCAGTGCCTGATGAGACCAAGCTTCAC	Cloning pGG-D-U3-OsU3-BbsI-ccdB-BbsI-E	pGG-D-OsU3-BbsI-ccdB-BbsI-E	Gibson assembly
2116	F_U4	GGCGCGGCCGCTAAGACAACACGCAAAGTCAGTAATTCATCCAGGTCACC	Cloning pGG-E-U4-OsU3-BbsI-ccdB-BbsI-F	pGG-E-OsU3-BbsI-ccdB-BbsI-F	Gibson assembly
2117	R_U4	GTTGTCTTAGCGGCCGCGCCAGGAGGTCAGGCAGTGAGACCAAGCTTCAC	Cloning pGG-E-U4-OsU3-BbsI-ccdB-BbsI-F	pGG-E-OsU3-BbsI-ccdB-BbsI-F	Gibson assembly
2118	F_U5	CCTTTACAACCTCACTCAAGTCCGTTAGAGAGTAATTCATCCAGGTCACC	Cloning pGG-F-U5-OsU3-BbsI-ccdB-BbsI-G	pGG-F-OsU3-BbsI-ccdB-BbsI-G	Gibson assembly
2119	R_U5	CTTGAGTGAGGTTGTAAAGGGAGTTGGCTCTAGTTGAGACCAAGCTTCAC	Cloning pGG-F-U5-OsU3-BbsI-ccdB-BbsI-G	pGG-F-OsU3-BbsI-ccdB-BbsI-G	Gibson assembly
4741	S1g1_F	TATATGAAGACCTGGCATATATGCAGGGACGTGGTGCGTTTTAGAGCTAGAAATAGC	Cloning pGG-A-Script1-entry1-B	pEN-2xTaU3	Golden Gate reaction (BbsI)
4742	S1g2_R	TATATGAAGACCTAAACGCCAGCTTTGACATCGCGCCTGCTTCTTGGTGCCGCGCCTC	Cloning pGG-A-Script1-entry1-B	pEN-2xTaU3	Golden Gate reaction (BbsI)
4743	S1g3_F	TATATGAAGACCTGGCACGGACGGGTCAGCCGGCACCGTTTTAGAGCTAGAAATAGC	Cloning pGG-B-Script1-entry2-C	pEN-2xTaU3	Golden Gate reaction (BbsI)
4744	S1g4_R	TATATGAAGACCTAAACAGGCCTCCCCTGTCCCGTCATGCTTCTTGGTGCCGCGCCTC	Cloning pGG-B-Script1-entry2-C	pEN-2xTaU3	Golden Gate reaction (BbsI)
4745	S1g5_F	TATATGAAGACCTGGCACGACGAGATCTTCACGGTGTGTTTTAGAGCTAGAAATAGC	Cloning pGG-C-Script1-entry3-D	pEN-2xTaU3	Golden Gate reaction (BbsI)
4746	S1g6_R	TATATGAAGACCTAAACTAACGGCCCGGCCGGCGCGGTGCTTCTTGGTGCCGCGCCTC	Cloning pGG-C-Script1-entry3-D	pEN-2xTaU3	Golden Gate reaction (BbsI)
4747	S1g7_F	TATATGAAGACCTGGCAAGGCAGGGGTAGTTCAGCGCGTTTTAGAGCTAGAAATAGC	Cloning pGG-D-Script1-entry4-E	pEN-2xTaU3	Golden Gate reaction (BbsI)
4748	S1g8_R	TATATGAAGACCTAAACCCGGACAGCTCCCTCCTCGATGCTTCTTGGTGCCGCGCCTC	Cloning pGG-D-Script1-entry4-E	pEN-2xTaU3	Golden Gate reaction (BbsI)
4749	S1g9_F	TATATGAAGACCTGGCAGGAGGGAGCCGTCCGGTGCCGTTTTAGAGCTAGAAATAGC	Cloning pGG-E-Script1-entry5-F	pEN-2xTaU3	Golden Gate reaction (BbsI)
4750	S1g10_R	TATATGAAGACCTAAACCACGGGCATTGGGCCGCCGTTGCTTCTTGGTGCCGCGCCTC	Cloning pGG-E-Script1-entry5-F	pEN-2xTaU3	Golden Gate reaction (BbsI)
4751	S1g11_F	TATATGAAGACCTGGCAGTACACCTCTGTGAGTGAGTGTTTTAGAGCTAGAAATAGC	Cloning pGG-F-Script1-entry6-G	pEN-2xTaU3	Golden Gate reaction (BbsI)
4752	S1g12_R	TATATGAAGACCTAAACATTGCAACATGGGAGTTATCTGCTTCTTGGTGCCGCGCCTC	Cloning pGG-F-Script1-entry6-G	pEN-2xTaU3	Golden Gate reaction (BbsI)
4753	S2g1_F	TATATGAAGACCTGGCAATAGCACTCTTCCATCTGACGTTTTAGAGCTAGAAATAGC	Cloning pGG-A-Script2-entry1-B	pEN-2xTaU3	Golden Gate reaction (BbsI)
4754	S2g2_R	TATATGAAGACCTAAACGACCGTGCTTGAGCGTCTCATGCTTCTTGGTGCCGCGCCTC	Cloning pGG-A-Script2-entry1-B	pEN-2xTaU3	Golden Gate reaction (BbsI)
4755	S2g3_F	TATATGAAGACCTGGCACTTGAGCGAGGTGAGCTTCAGTTTTAGAGCTAGAAATAGC	Cloning pGG-B-Script2-entry2-C	pEN-2xTaU3	Golden Gate reaction (BbsI)
4756	S2g4_R	TATATGAAGACCTAAACAAAGGGTAACAGCCACAACATGCTTCTTGGTGCCGCGCCTC	Cloning pGG-B-Script2-entry2-C	pEN-2xTaU3	Golden Gate reaction (BbsI)
4757	S2g5_F	TATATGAAGACCTGGCATTCCTGGACCGCGTGAGCGCGTTTTAGAGCTAGAAATAGC	Cloning pGG-C-Script2-entry3-D	pEN-2xTaU3	Golden Gate reaction (BbsI)
4758	S2g6_R	TATATGAAGACCTAAACTCCTGACCCGGTTCAGGAAGTGCTTCTTGGTGCCGCGCCTC	Cloning pGG-C-Script2-entry3-D	pEN-2xTaU3	Golden Gate reaction (BbsI)
4759	S2g7_F	TATATGAAGACCTGGCATGTTCATGGCAGCTCTAGGCGTTTTAGAGCTAGAAATAGC	Cloning pGG-D-Script2-entry4-E	pEN-2xTaU3	Golden Gate reaction (BbsI)
4760	S2g8_R	TATATGAAGACCTAAACCCATGAACAGGTCCGAGTTCTGCTTCTTGGTGCCGCGCCTC	Cloning pGG-D-Script2-entry4-E	pEN-2xTaU3	Golden Gate reaction (BbsI)
4761	S2g9_F	TATATGAAGACCTGGCACACCCAATGCTGCGTAGAACGTTTTAGAGCTAGAAATAGC	Cloning pGG-E-Script2-entry5-F	pEN-2xTaU3	Golden Gate reaction (BbsI)
4762	S2g10_R	TATATGAAGACCTAAACCTCAAGCACGTGCGGGGCCTTGCTTCTTGGTGCCGCGCCTC	Cloning pGG-E-Script2-entry5-F	pEN-2xTaU3	Golden Gate reaction (BbsI)
4763	S2g11_F	TATATGAAGACCTGGCATCCTCTGCAGGTTGTGGACCGTTTTAGAGCTAGAAATAGC	Cloning pGG-F-Script2-entry6-G	pEN-2xTaU3	Golden Gate reaction (BbsI)
4764	S2g12_R	TATATGAAGACCTAAACCTGCAAGTTGCTCCGCCCAATGCTTCTTGGTGCCGCGCCTC	Cloning pGG-F-Script2-entry6-G	pEN-2xTaU3	Golden Gate reaction (BbsI)
4765	S3g1_F	TATATGAAGACCTGGCACTCGCGGTCTGGGCCGCTCCGTTTTAGAGCTAGAAATAGC	Cloning pGG-A-Script2-entry1-B	pEN-2xTaU3	Golden Gate reaction (BbsI)
4766	S3g2_R	TATATGAAGACCTAAACAGTTGCTCGCGGTGACGACATGCTTCTTGGTGCCGCGCCTC	Cloning pGG-A-Script2-entry1-B	pEN-2xTaU3	Golden Gate reaction (BbsI)
4767	S3g3_F	TATATGAAGACCTGGCACGCAGAAGCTGTGCTCGCGAGTTTTAGAGCTAGAAATAGC	Cloning pGG-B-Script3-entry2-C	pEN-2xTaU3	Golden Gate reaction (BbsI)
4768	S3g4_R	TATATGAAGACCTAAACGCGATTCGCAGAGGCGTAAGTGCTTCTTGGTGCCGCGCCTC	Cloning pGG-B-Script3-entry2-C	pEN-2xTaU3	Golden Gate reaction (BbsI)
4769	S3g5_F	TATATGAAGACCTGGCACTCCTCACGGACGCCACCTGGTTTTAGAGCTAGAAATAGC	Cloning pGG-C-Script3-entry3-D	pEN-2xTaU3	Golden Gate reaction (BbsI)
4770	S3g6_R	TATATGAAGACCTAAACGCGACCACGAGGAGGTCGGGTGCTTCTTGGTGCCGCGCCTC	Cloning pGG-C-Script3-entry3-D	pEN-2xTaU3	Golden Gate reaction (BbsI)
4771	S3g7_F	TATATGAAGACCTGGCACCGCACGCTCGCGCTGCAGAGTTTTAGAGCTAGAAATAGC	Cloning pGG-D-Script3-entry4-E	pEN-2xTaU3	Golden Gate reaction (BbsI)
4772	S3g8_R	TATATGAAGACCTAAACCGAGCTGCCGGTTCATACCGTGCTTCTTGGTGCCGCGCCTC	Cloning pGG-D-Script3-entry4-E	pEN-2xTaU3	Golden Gate reaction (BbsI)
4773	S3g9_F	TATATGAAGACCTGGCAGGCTCGCCCATGCACTTCTTGTTTTAGAGCTAGAAATAGC	Cloning pGG-E-Script3-entry5-F	pEN-2xTaU3	Golden Gate reaction (BbsI)
4774	S3g10_R	TATATGAAGACCTAAACCAGGTTCTGGCACGAGTGTCTGCTTCTTGGTGCCGCGCCTC	Cloning pGG-E-Script3-entry5-F	pEN-2xTaU3	Golden Gate reaction (BbsI)
4775	S3g11_F	TATATGAAGACCTGGCACATGGAGGATATCCACGCACGTTTTAGAGCTAGAAATAGC	Cloning pGG-F-Script3-entry6-G	pEN-2xTaU3	Golden Gate reaction (BbsI)
4776	S3g12_R	TATATGAAGACCTAAACGTGGACTGAGTCAATGACCTTGCTTCTTGGTGCCGCGCCTC	Cloning pGG-F-Script3-entry6-G	pEN-2xTaU3	Golden Gate reaction (BbsI)
4777	S4g1_F	TATATGAAGACCTGGCAAGGCGCGCACGGGCTGTCGAGTTTTAGAGCTAGAAATAGC	Cloning pGG-A-Script4-entry1-B	pEN-2xTaU3	Golden Gate reaction (BbsI)
4778	S4g2_R	TATATGAAGACCTAAACCTGGCCAAGCCGAAGTGCTGTGCTTCTTGGTGCCGCGCCTC	Cloning pGG-A-Script4-entry1-B	pEN-2xTaU3	Golden Gate reaction (BbsI)
4779	S4g3_F	TATATGAAGACCTGGCACAGCTCCTGGCTGTGTCCGCGTTTTAGAGCTAGAAATAGC	Cloning pGG-B-Script4-entry2-C	pEN-2xTaU3	Golden Gate reaction (BbsI)
4780	S4g4_R	TATATGAAGACCTAAACCAGGACCTCATGGTTGGGCATGCTTCTTGGTGCCGCGCCTC	Cloning pGG-B-Script4-entry2-C	pEN-2xTaU3	Golden Gate reaction (BbsI)
4781	S4g5_F	TATATGAAGACCTGGCACCAGTTCCCGCCGCAAGGGCGTTTTAGAGCTAGAAATAGC	Cloning pGG-C-Script4-entry3-D	pEN-2xTaU3	Golden Gate reaction (BbsI)
4782	S4g6_R	TATATGAAGACCTAAACGGCGAGTCTTGGACCGGTACTGCTTCTTGGTGCCGCGCCTC	Cloning pGG-C-Script4-entry3-D	pEN-2xTaU3	Golden Gate reaction (BbsI)
4783	S4g7_F	TATATGAAGACCTGGCA[illegible]GAAATAGC	Cloning pGG-D-Script4-entry4-E	pEN-2xTaU3	Golden Gate reaction (BbsI)
4784	S4g8_R	TATATGAAGACCTAAACAG[illegible]CAGGGACGGATGTGCTTCTTGGTGCCGCGCCTC	Cloning pGG-D-Script4-entry4-E	pEN-2xTaU3	Golden Gate reaction (BbsI)
4785	S4g9_F	TATATGAAGACCTGGCAGGACCTCCGGATCCTCGACCGTTTTAGAGCTAGAAATAGC	Cloning pGG-E-Script4-entry5-F	pEN-2xTaU3	Golden Gate reaction (BbsI)
4786	S4g10_R	TATATGAAGACCTAAACCTCCTGCGAACAGGACAGAATGCTTCTTGGTGCCGCGCCTC	Cloning pGG-E-Script4-entry5-F	pEN-2xTaU3	Golden Gate reaction (BbsI)
4787	S4g11_F	TATATGAAGACCTGGCACACTGGACATATGAACAAACGTTTTAGAGCTAGAAATAGC	Cloning pGG-F-Script4-entry6-G	pEN-2xTaU3	Golden Gate reaction (BbsI)
4788	S4g12_R	TATATGAAGACCTAAACCCTCTCAATGGAACAAAGAATGCTTCTTGGTGCCGCGCCTC	Cloning pGG-F-Script4-entry6-G	pEN-2xTaU3	Golden Gate reaction (BbsI)
4789	S5g1_F	TATATGAAGACCTGGCAGCATGTGATGGACCGTCAGGGTTTTAGAGCTAGAAATAGC	Cloning pGG-A-Script5-entry1-B	pEN-2xTaU3	Golden Gate reaction (BbsI)
4790	S5g2_R	TATATGAAGACCTAAACTATCATCGGCGGCCCCAGCCTGCTTCTTGGTGCCGCGCCTC	Cloning pGG-A-Script5-entry1-B	pEN-2xTaU3	Golden Gate reaction (BbsI)
4791	S5g3_F	TATATGAAGACCTGGCAACAGACACGGCGAGCCCCGTGTTTTAGAGCTAGAAATAGC	Cloning pGG-B-Script5-entry2-C	pEN-2xTaU3	Golden Gate reaction (BbsI)
4792	S5g4_R	TATATGAAGACCTAAACCCGGGCGTTCCCCCATTTCTTGCTTCTTGGTGCCGCGCCTC	Cloning pGG-B-Script5-entry2-C	pEN-2xTaU3	Golden Gate reaction (BbsI)
4793	S5g5_F	TATATGAAGACCTGGCAGCGGGCCTTCCGGCGGCAACGTTTTAGAGCTAGAAATAGC	Cloning pGG-C-Script5-entry3-D	pEN-2xTaU3	Golden Gate reaction (BbsI)
4794	S5g6_R	TATATGAAGACCTAAACTTTAGGCTCTCCATTCTTCCTGCTTCTTGGTGCCGCGCCTC	Cloning pGG-C-Script5-entry3-D	pEN-2xTaU3	Golden Gate reaction (BbsI)
4795	S5g7_F	TATATGAAGACCTGGCAGGACTCGGTATAGAGTCTCAGTTTTAGAGCTAGAAATAGC	Cloning pGG-D-Script5-entry4-E	pEN-2xTaU3	Golden Gate reaction (BbsI)
4796	S5g8_R	TATATGAAGACCTAAACTGTACCGTGTCCTGAAGCACTGCTTCTTGGTGCCGCGCCTC	Cloning pGG-D-Script5-entry4-E	pEN-2xTaU3	Golden Gate reaction (BbsI)
4797	S5g9_F	TATATGAAGACCTGGCACACATAATATCGACTACGATGTTTTAGAGCTAGAAATAGC	Cloning pGG-E-Script5-entry5-F	pEN-2xTaU3	Golden Gate reaction (BbsI)
4798	S5g10_R	TATATGAAGACCTAAACACGTCCCCGCGCAGGTGTGGTGCTTCTTGGTGCCGCGCCTC	Cloning pGG-E-Script5-entry5-F	pEN-2xTaU3	Golden Gate reaction (BbsI)
4763	S2g11_F	TATATGAAGACCTGGCATCCTCTGCAGGTTGTGGACCGTTTTAGAGCTAGAAATAGC	Cloning pGG-F-Script5-entry6-G	pEN-2xTaU3	Golden Gate reaction (BbsI)
4800	S5g12_R	TATATGAAGACCTAAACGCGGACTTGGGCTTCCTGCTTGCTTCTTGGTGCCGCGCCTC	Cloning pGG-F-Script5-entry6-G	pEN-2xTaU3	Golden Gate reaction (BbsI)
1651	M13F43	AGGGTTTTCCCAGTCACGACGTT	Sequencing Golden Gate entry		
1652	PexR	CAGGCTTTACACTTTATGCTTCCGGC	Sequencing Golden Gate entry		
2118	F_U5	CCTTTACAACCTCACTCAAGTCCGTTAGAGAGTAATTCATCCAGGTCACC	Colony PCR Agrobacterium expression vectors		
1790	35SR1	CCTCTCTAACCATCTGTGGGTTAGC	Colony PCR Agrobacterium expression vectors		

Supplemental Table 4: Primers used for plasmid building and sequencing.

Parsed Citations

Anzalone AV, Koblan LW, and Liu DR. (2020). Genome editing with CRISPR-Cas nucleases, base editors, transposases and prime editors. Nat. Biotechnol. 38: 824-844
Google Scholar: Author Only Title Only Author and Title

Ashikari M, Sakakibara H, Lin S, Yamamoto T, Takashi T, Nishimura A, Angeles ER, Qian Q, Kitano H, and Matsuoka M. (2005). Cytokinin oxidase regulates rice grain production. Science 309: 741-745
Google Scholar: Author Only Title Only Author and Title

Bai M, Yuan J, Kuang H, Gong P, Li S, Zhang Z, Liu B, Sun J, Yang M, Yang L, et al. (2020). Generation of a multiplex mutagenesis population via pooled CRISPR-Cas9 in soya bean. Plant Biotechnol. J. 18: 721-731
Google Scholar: Author Only Title Only Author and Title

Bartrina I, Otto E, Strnad M, Werner T, and Schmülling T. (2011). Cytokinin regulates the activity of reproductive meristems, flower organ size, ovule formation, and thus seed yield in Arabidopsis thaliana. Plant Cell 23: 69-80
Google Scholar: Author Only Title Only Author and Title

Baute J, Herman D, Coppens F, De Block J, Slabbinck B, Dell'Acqua M, Pè ME, Maere S, Nelissen H, and Inzé D. (2015). Correlation analysis of the transcriptome of growing leaves with mature leaf parameters in a maize RIL population. Genome Biol. 16: 168
Google Scholar: Author Only Title Only Author and Title

Baute J, Herman D, Coppens F, De Block J, Slabbinck B, Dell'Acqua M, Pè ME, Maere S, Nelissen H, and Inzé D. (2016). Combined large-scale phenotyping and transcriptomics in maize reveals a robust growth regulatory network. Plant Physiol. 170: 1848-1867
Google Scholar: Author Only Title Only Author and Title

Berendzen K, Searle I, Ravenscroft D, Koncz C, Batschauer A, Coupland G, Somssich IE, and Ülker B. (2005). A rapid and versatile combined DNA/RNA extraction protocol and its application to the analysis of a novel DNA marker set polymorphic between Arabidopsis thaliana ecotypes Col-0 and Landsberg erecta. Plant Methods 1: 4
Google Scholar: Author Only Title Only Author and Title

Bhat JA, Yu D, Bohra A, Ganie SA, and Varshney RK. (2021). Features and applications of haplotypes in crop breeding. Commun. Biol. 4: 1266
Google Scholar: Author Only Title Only Author and Title

Bloch D, Puli MR, Mosquna A, and Yalovsky S. (2019). Abiotic stress modulates root patterning via ABA-regulated microRNA expression in the endodermis initials. Development 146: dev177097
Google Scholar: Author Only Title Only Author and Title

Borg M, and Berger F. (2015). Chromatin remodelling during male gametophyte development. Plant J. 83: 177-188
Google Scholar: Author Only Title Only Author and Title

Brás TA, Seixas J, Carvalhais N, and Jägermeyr J. (2021). Severity of drought and heatwave crop losses tripled over the last five decades in Europe. Environ. Res. Lett. 16: 065012
Google Scholar: Author Only Title Only Author and Title

Cao L, Wang S, Venglat P, Zhao L, Cheng Y, Ye S, Qin Y, Datla R, Zhou Y, and Wang H. (2018). Arabidopsis ICK/KRP cyclin-dependent kinase inhibitors function to ensure the formation of one megaspore mother cell and one functional megaspore per ovule. PLoS Genet. 14: e1007230
Google Scholar: Author Only Title Only Author and Title

Chaikam V, Molenaar W, Melchinger AE, and Boddupalli PM. (2019). Doubled haploid technology for line development in maize: technical advances and prospects. Theor. Appl. Genet. 132: 3227-3243
Google Scholar: Author Only Title Only Author and Title

Cheng Y, Cao L, Wang S, Li Y, Shi X, Liu H, Li L, Zhang Z, Fowke LC, Wang H, et al. (2013). Downregulation of multiple CDK inhibitor ICK/KRP genes upregulates the E2F pathway and increases cell proliferation, and organ and seed sizes in Arabidopsis. Plant J. 75: 642-655
Google Scholar: Author Only Title Only Author and Title

Colombo N, and Favret EA. (1996). The effect of gibberellic acid on male fertility in bread wheat. Euphytica 91: 297-303
Google Scholar: Author Only Title Only Author and Title

Coussens G, Aesaert S, Verelst W, Demeulenaere M, De Buck S, Njuguna E, Inzé D, and Van Lijsebettens M. (2012). Brachypodium distachyon promoters as efficient building blocks for transgenic research in maize. J. Exp. Bot. 63: 4263-4273
Google Scholar: Author Only Title Only Author and Title

Czesnick H, and Lenhard M. (2015). Size control in plants-lessons from leaves and flowers. Cold Spring Harb. Perspect. Biol. 7:

a019190
Google Scholar: Author Only Title Only Author and Title

Decaestecker W, Andrade Buono R, Pfeiffer ML, Vangheluwe N, Jourquin J, Karimi M, Van Isterdael G, Beeckman T, Nowack MK, and Jacobs TB. (2019). CRISPR-TSKO: a technique for efficient mutagenesis in specific cell types, tissues, or organs in Arabidopsis. Plant Cell 31: 2868-2887
Google Scholar: Author Only Title Only Author and Title

Doll NM, Gilles LM, Gerentes M-F, Richard C, Just J, Fierlej Y, Borrelli VMG, Gendrot G, Ingram GC, Rogowsky PM, et al. (2019). Single and multiple gene knockouts by CRISPR–Cas9 in maize. Plant Cell Rep. 38: 487-501
Google Scholar: Author Only Title Only Author and Title

Elias F, Muleta D, and Woyessa D. (2016). Effects of phosphate solubilizing fungi on growth and yield of haricot bean (Phaseolus vulgaris L.) plants. J. Agric. Sci. 8: 204-218
Google Scholar: Author Only Title Only Author and Title

Gaillochet C, Develtere W, and Jacobs TB. (2021). CRISPR screens in plants: approaches, guidelines, and future prospects. Plant Cell 33: 794-813
Google Scholar: Author Only Title Only Author and Title

Gong P, Bontinck M, Demuynck K, De Block J, Gevaert K, Eeckhout D, Persiau G, Aesaert S, Coussens G, Van Lijsebettens M, et al. (2022). SAMBA controls cell division rate during maize development. Plant Physiol. 188: 411-424
Google Scholar: Author Only Title Only Author and Title

Gong R, Cao H, Zhang J, Xie K, Wang D, and Yu S. (2018). Divergent functions of the GAGA-binding transcription factor family in rice. Plant J. 94: 32-47
Google Scholar: Author Only Title Only Author and Title

Gonzalez N, Vanhaeren H, and Inzé D. (2012). Leaf size control: complex coordination of cell division and expansion. Trends Plant Sci. 17: 332-340
Google Scholar: Author Only Title Only Author and Title

Hai NN, Chuong NN, Tu NHC, Kisiala A, Hoang XLT, and Thao NP. (2020). Role and regulation of cytokinins in plant response to drought stress. Plants 9: 422
Google Scholar: Author Only Title Only Author and Title

He Z, Wu J, Sun X, and Dai M. (2019). The maize clade A PP2C phosphatases play critical roles in multiple abiotic stress responses. Int. J. Mol. Sci. 20: 3573
Google Scholar: Author Only Title Only Author and Title

Houbaert A, Zhang C, Tiwari M, Wang K, de Marcos Serrano A, Savatin DV, Urs MJ, Zhiponova MK, Gudesblat GE, Vanhoutte I, et al. (2018). POLAR-guided signalling complex assembly and localization drive asymmetric cell division. Nature 563: 574-578
Google Scholar: Author Only Title Only Author and Title

Huang Y, Wang X, Ge S, and Rao G-Y. (2015). Divergence and adaptive evolution of the gibberellin oxidase genes in plants. BMC Evol. Biol. 15: 207
Google Scholar: Author Only Title Only Author and Title

Hwang BG, Ryu J, and Lee SJ. (2016). Vulnerability of protoxylem and metaxylem vessels to embolisms and radial refilling in a vascular bundle of maize leaves. Front. Plant Sci. 7: 941
Google Scholar: Author Only Title Only Author and Title

Ikeda A, Ueguchi-Tanaka M, Sonoda Y, Kitano H, Koshioka M, Futsuhara Y, Matsuoka M, and Yamaguchi J. (2001). slender rice, a constitutive gibberellin response mutant, is caused by a null mutation of the SLR1 gene, an ortholog of the height-regulating gene GAI/RGA/RHT/D8. Plant Cell 13: 999-1010
Google Scholar: Author Only Title Only Author and Title

Impens L, Jacobs TB, Nelissen H, Inz2 D, and Pauwels L. (2022). Mini-Review: Transgenerational CRISPR/Cas9 gene editing in plants. Frontiers in Genome Editing 4: 825042
Google Scholar: Author Only Title Only Author and Title

Itoh H, Shimada A, Ueguchi-Tanaka M, Kamiya N, Hasegawa Y, Ashikari M, and Matsuoka M. (2005). Overexpression of a GRAS protein lacking the DELLA domain confers altered gibberellin responses in rice. Plant J. 44: 669-679
Google Scholar: Author Only Title Only Author and Title

Jacobs TB, Zhang N, Patel D, and Martin GB. (2017). Generation of a collection of mutant tomato lines using pooled CRISPR libraries. Plant Physiol. 174: 2023-2037
Google Scholar: Author Only Title Only Author and Title

Jacquier NMA, Gilles LM, Pyott DE, Martinant J-P, Rogowsky PM, and Widiez T. (2020). Puzzling out plant reproduction by haploid

induction for innovations in plant breeding. Nat. Plants 6: 610-619
Google Scholar: Author Only Title Only Author and Title

Jiao Y, Peluso P, Shi J, Liang T, Stitzer MC, Wang B, Campbell MS, Stein JC, Wei X, Chin C-S, et al. (2017). Improved maize reference genome with single-molecule technologies. Nature 546: 524-527
Google Scholar: Author Only Title Only Author and Title

Karimi M, Inzé D, Van Lijsebettens M, and Hilson P. (2013). Gateway vectors for transformation of cereals. Trends Plant Sci. 18: 1-4
Google Scholar: Author Only Title Only Author and Title

Knott GJ, and Doudna JA. (2018). CRISPR-Cas guides the future of genetic engineering. Science 361: 866-869
Google Scholar: Author Only Title Only Author and Title

Koyama T, Sato F, and Ohme-Takagi M. (2017). Roles of miR319 and TCP transcription factors in leaf development. Plant Physiol. 175: 874-885
Google Scholar: Author Only Title Only Author and Title

Lampropoulos A, Sutikovic Z, Wenzl C, Maegele I, Lohmann JU, and Forner J. (2013). GreenGate - A novel, versatile, and efficient cloning system for plant transgenesis. PLoS ONE 8: e83043
Google Scholar: Author Only Title Only Author and Title

Lan J, and Qin G. (2020). The regulation of CIN-like TCP transcription factors. Int. J. Mol. Sci. 21: 4498
Google Scholar: Author Only Title Only Author and Title

Lawit SJ, Wych HM, Xu D, Kundu S, and Tomes DT. (2010). Maize DELLA Proteins dwarf plant8 and dwarf plant9 as Modulators of Plant Development. Plant and Cell Physiology 51: 1854-1868
Google Scholar: Author Only Title Only Author and Title

Li C, Hao M, Wang W, Wang H, Chen F, Chu W, Zhang B, Mei D, Cheng H, and Hu Q. (2018). An efficient CRISPR/Cas9 platform for rapidly generating simultaneous mutagenesis of multiple gene homoeologs in allotetraploid oilseed rape. Front. Plant Sci. 9: 442
Google Scholar: Author Only Title Only Author and Title

Li J, Wang Z, He G, Ma L, and Deng XW. (2020). CRISPR/Cas9-mediated disruption of TaNP1 genes results in complete male sterility in bread wheat. J. Genet. Genomics 47: 263-272
Google Scholar: Author Only Title Only Author and Title

Li N, and Li Y. (2016). Signaling pathways of seed size control in plants. Curr. Opin. Plant Biol. 33: 23-32
Google Scholar: Author Only Title Only Author and Title

Li W, Herrera-Estrella L, and Tran L-SP. (2016). The yin–yang of cytokinin homeostasis and drought acclimation/adaptation. Trends Plant Sci. 21: 548-550
Google Scholar: Author Only Title Only Author and Title

Li Y, Shan X, Jiang Z, Zhao L, and Jin F. (2021). Genome-wide identification and expression analysis of the GA2ox gene family in maize (Zea mays L.) under various abiotic stress conditions. Plant Physiol. Biochem. 166: 621-633
Google Scholar: Author Only Title Only Author and Title

Liebsch D, and Palatnik JF. (2020). MicroRNA miR396, GRF transcription factors and GIF co-regulators: a conserved plant growth regulatory module with potential for breeding and biotechnology. Curr. Opin. Plant Biol. 53: 31-42
Google Scholar: Author Only Title Only Author and Title

Liu H-J, Jian L, Xu J, Zhang Q, Zhang M, Jin M, Peng Y, Yan J, Han B, Liu J, et al. (2020). High-throughput CRISPR/Cas9 mutagenesis streamlines trait gene identification in maize. Plant Cell 32: 1397-1413
Google Scholar: Author Only Title Only Author and Title

Liu L, Gallagher J, Arevalo ED, Chen R, Skopelitis T, Wu Q, Bartlett M, and Jackson D. (2021). Enhancing grain-yield-related traits by CRISPR–Cas9 promoter editing of maize CLE genes. Nat. Plants 7: 287-294
Google Scholar: Author Only Title Only Author and Title

Long SP, Marshall-Colon A, and Zhu X-G. (2015). Meeting the global food demand of the future by engineering crop photosynthesis and yield potential. Cell 161: 56-66
Google Scholar: Author Only Title Only Author and Title

Lu Y, Ye X, Guo R, Huang J, Wang W, Tang J, Tan L, Zhu J-k, Chu C, and Qian Y. (2017). Genome-wide targeted mutagenesis in rice using the CRISPR/Cas9 system. Mol. Plant 10: 1242-1245
Google Scholar: Author Only Title Only Author and Title

McConnell JR, Emery J, Eshed Y, Bao N, Bowman J, and Barton MK. (2001). Role of PHABULOSA and PHAVOLUTA in determining radial patterning in shoots. Nature 411: 709-713
Google Scholar: Author Only Title Only Author and Title

Meng X, Yu H, Zhang Y, Zhuang F, Song X, Gao S, Gao C, and Li J. (2017). Construction of a genome-wide mutant library in rice using CRISPR/Cas9. Mol. Plant 10: 1238-1241
Google Scholar: Author Only Title Only Author and Title

Mickelbart MV, Hasegawa PM, and Bailey-Serres J. (2015). Genetic mechanisms of abiotic stress tolerance that translate to crop yield stability. Nat. Rev. Genet. 16: 237-251
Google Scholar: Author Only Title Only Author and Title

Miculan M, Nelissen H, Hassen MB, Marroni F, Inzé D, Pè ME, and Dell'Acqua M. (2021). A forward genetics approach integrating genome-wide association study and expression quantitative trait locus mapping to dissect leaf development in maize (Zea mays). Plant J. 107: 1056-1071
Google Scholar: Author Only Title Only Author and Title

Mills A, Allsman L, Leon S, and Rasmussen C. (2020). Using seed chipping to genotype maize kernels. Bio-Protocol 101: e3553
Google Scholar: Author Only Title Only Author and Title

Nelissen H, Rymen B, Jikumaru Y, Demuynck K, Van Lijsebettens M, Kamiya Y, Inzé D, and Beemster GTS. (2012). A local maximum in gibberellin levels regulates maize leaf growth by spatial control of cell division. Curr. Biol. 22: 1183-1187
Google Scholar: Author Only Title Only Author and Title

Nelissen H, Eeckhout D, Demuynck K, Persiau G, Walton A, van Bel M, Vervoort M, Candaele J, De Block J, Aesaert S, et al. (2015). Dynamic changes in ANGUSTIFOLIA3 complex composition reveal a growth regulatory mechanism in the maize leaf. Plant Cell 27: 1605-1619
Google Scholar: Author Only Title Only Author and Title

Nuccio ML, Paul M, Bate NJ, Cohn J, and Cutler SR. (2018). Where are the drought tolerant crops? An assessment of more than two decades of plant biotechnology effort in crop improvement. Plant Sci. 273: 110-119
Google Scholar: Author Only Title Only Author and Title

Paul BK, Frelat R, Birnholz C, Ebong C, Gahigi A, Groot JCJ, Herrero M, Kagabo DM, Notenbaert A, Vanlauwe B, et al. (2018). Agricultural intensification scenarios, household food availability and greenhouse gas emissions in Rwanda: Ex-ante impacts and trade-offs. Agric. Syst. 163: 16-26
Google Scholar: Author Only Title Only Author and Title

Poland J, and Rutkoski J. (2016). Advances and challenges in genomic selection for disease resistance. Annu. Rev. Phytopathol. 54: 79-98
Google Scholar: Author Only Title Only Author and Title

Qin F, Kodaira K-S, Maruyama K, Mizoi J, Tran L-SP, Fujita Y, Morimoto K, Shinozaki K, and Yamaguchi-Shinozaki K. (2011). SPINDLY , a negative regulator of gibberellic acid signaling, is involved in the plant abiotic stress response. Plant Physiol. 157: 1900-1913
Google Scholar: Author Only Title Only Author and Title

Ramadan M, Alariqi M, Ma Y, Li Y, Liu Z, Zhang R, Jin S, Min L, and Zhang X. (2021). Efficient CRISPR/Cas9 mediated pooled-sgRNAs assembly accelerates targeting multiple genes related to male sterility in cotton. Plant Methods 17: 16
Google Scholar: Author Only Title Only Author and Title

Rasheed A, Hao Y, Xia X, Khan A, Xu Y, Varshney RK, and He Z. (2017). Crop breeding chips and genotyping platforms: progress, challenges, and perspectives. Mol. Plant 10: 1047-1064
Google Scholar: Author Only Title Only Author and Title

Rida S, Maafi O, López-Malvar A, Revilla P, Riache M, and Djemel A. (2021). Genetics of germination and seedling traits under drought stress in a MAGIC population of maize. Plants 10: 1786
Google Scholar: Author Only Title Only Author and Title

Rodríguez-Leal D, Lemmon ZH, Man J, Bartlett ME, and Lippman ZB. (2017). Engineering quantitative trait variation for crop improvement by genome editing. Cell 171: 470-480.e478
Google Scholar: Author Only Title Only Author and Title

Sarvepalli K, and Nath U. (2018). CIN-TCP transcription factors: transiting cell proliferation in plants. IUBMB Life 70: 718-731
Google Scholar: Author Only Title Only Author and Title

Schaumont D, Veeckman E, Van der Jeugt F, Haegeman A, Glabeke Sv, Bawin Y, Lukasiewicz J, Blugeon S, Barre P, de la O. Leyva-Pérez M, et al. (2022). Stack Mapping Anchor Points (SMAP): a versatile suite of tools for read-backed haplotyping. bioRxiv 2022.03.10.483555
Google Scholar: Author Only Title Only Author and Title

Simmons CR, Lafitte HR, Reimann KS, Brugière N, Roesler K, Albertsen MC, Greene TW, and Habben JE. (2021). Successes and insights of an industry biotech program to enhance maize agronomic traits. Plant Sci. 307: 110899
Google Scholar: Author Only Title Only Author and Title

Snowdon RJ, Wittkop B, Chen T-W, and Stahl A. (2021). Crop adaptation to climate change as a consequence of long-term breeding. Theor. Appl. Genet. 134: 1613-1623
Google Scholar: Author Only Title Only Author and Title

Sun X, Cahill J, Van Hautegem T, Feys K, Whipple C, Novák O, Delbare S, Versteele C, Demuynck K, De Block J, et al. (2017). Altered expression of maize PLASTOCHRON1 enhances biomass and seed yield by extending cell division duration. Nat. Commun. 8: 14752
Google Scholar: Author Only Title Only Author and Title

Teixeira FF, and Guimarães CT. (2021). Chapter 5 - Maize genetic resources and pre-breeding. In Wild Germplasm for Genetic Improvement in Crop Plants, M.T. Azhar and S.H. Wani, eds (London, United Kingdom: Academic Press, Elsevier), pp. 81-99
Google Scholar: Author Only Title Only Author and Title

Torella JP, Lienert F, Boehm CR, Chen J-H, Way JC, and Silver PA. (2014). Unique nucleotide sequence–guided assembly of repetitive DNA parts for synthetic biology applications. Nat. Protoc. 9: 2075-2089
Google Scholar: Author Only Title Only Author and Title

Vanhaeren H, Nam Y-J, De Milde L, Chae E, Storme V, Weigel D, Gonzalez N, and Inzé D. (2017). Forever young: the role of ubiquitin receptor DA1 and E3 ligase Big Brother in controlling leaf growth and development. Plant Physiol. 173: 1269-1282
Google Scholar: Author Only Title Only Author and Title

Vanhaeren H, Gonzalez N, Coppens F, De Milde L, Van Daele T, Vermeersch M, Eloy NB, Storme V, and Inzé D. (2014). Combining growth-promoting genes leads to positive epistasis in Arabidopsis thaliana. eLife 3: e02252
Google Scholar: Author Only Title Only Author and Title

Vats S, Kumawat S, Kumar V, Patil GB, Joshi T, Sonah H, Sharma TR, and Deshmukh R. (2019). Genome editing in plants: exploration of technological advancements and challenges. Cells 8: 1386
Google Scholar: Author Only Title Only Author and Title

Verbraeken L, Wuyts N, Mertens S, Cannoot B, Maleux K, Demuynck K, De Block J, Merchie J, Dhondt S, Bonaventure G, et al. (2021). Drought affects the rate and duration of organ growth but not inter-organ growth coordination. Plant Physiol. 186: 1336-1353
Google Scholar: Author Only Title Only Author and Title

Vercruysse J, Baekelandt A, Gonzalez N, and Inzé D. (2020). Molecular networks regulating cell division during Arabidopsis leaf growth. J. Exp. Bot. 71: 2365-2378
Google Scholar: Author Only Title Only Author and Title

Voorend W, Nelissen H, Vanholme R, De Vliegher A, Van Breusegem F, Boerjan W, Roldán-Ruiz I, Muylle H, and Inzé D. (2016). Overexpression of GA20-OXIDASE1 impacts plant height, biomass allocation and saccharification efficiency in maize. Plant Biotechnol. J. 14: 997–1007
Google Scholar: Author Only Title Only Author and Title

Voss-Fels K, and Snowdon RJ. (2016). Understanding and utilizing crop genome diversity via high-resolution genotyping. Plant Biotechnol. J. 14: 1086-1094
Google Scholar: Author Only Title Only Author and Title

Wang B, Li N, Huang S, Hu J, Wang Q, Tang Y, Yang T, Asmutola P, Wang J, and Yu Q. (2021). Enhanced soluble sugar content in tomato fruit using CRISPR/Cas9-mediated SlINVINH1 and SlVPE5 gene editing. PeerJ 9: e12478
Google Scholar: Author Only Title Only Author and Title

Wang H-Q, Liu P, Zhang J-W, Zhao B, and Ren B-Z. (2020). Endogenous hormones inhibit differentiation of young ears in maize (Zea mays L.) under heat stress. Front. Plant Sci. 11: 533046
Google Scholar: Author Only Title Only Author and Title

Wang H, and Qin F. (2017). Genome-wide association study reveals natural variations contributing to drought resistance in crops. Front. Plant Sci. 8: 1110
Google Scholar: Author Only Title Only Author and Title

Winkler RG, and Freeling M. (1994). Physiological genetics of the dominant gibberellin-nonresponsive maize dwarfs, Dwarf8 and Dwarf9. Planta 193: 341-348
Google Scholar: Author Only Title Only Author and Title

Wu L, Zhang D, Xue M, Qian J, He Y, and Wang S. (2014). Overexpression of the maize GRF10, an endogenous truncated growth-regulating factor protein, leads to reduction in leaf size and plant height. J. Integr. Plant Biol. 56: 1053-1063
Google Scholar: Author Only Title Only Author and Title

Xiao Y, Tong H, Yang X, Xu S, Pan Q, Qiao F, Raihan MS, Luo Y, Liu H, Zhang X, et al. (2016). Genome-wide dissection of the maize ear genetic architecture using multiple populations. New Phytol. 210: 1095-1106
Google Scholar: Author Only Title Only Author and Title

Xing H-L, Dong L, Wang Z-P, Zhang H-Y, Han C-Y, Liu B, Wang X-C, and Chen Q-J. (2014). A CRISPR/Cas9 toolkit for multiplex genome editing in plants. BMC Plant Biol. 14: 327

Google Scholar: Author Only Title Only Author and Title

Zhang X, and Cai X. (2011). Climate change impacts on global agricultural land availability. Environ. Res. Lett. 6: 014014

Google Scholar: Author Only Title Only Author and Title

Zhang Y, Malzahn AA, Sretenovic S, and Qi Y. (2019). The emerging and uncultivated potential of CRISPR technology in plant science. Nat. Plants 5: 778-794

Google Scholar: Author Only Title Only Author and Title